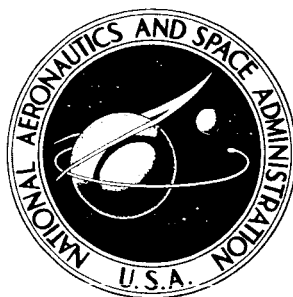


NASA CONTRACTOR REPORT



NASA CR-248

NASA CR-248

FACILITY FORM 502

N65-27396	
(ACCESSION NUMBER)	(THRU)
76	1
(PAGES)	(CODE)
(NASA CR OR TMX OR AD NUMBER)	52
	(CATEGORY)

GPO PRICE \$ _____

CPST/OTS PRICE(S) \$ 300

Hard copy (HC) _____

Microfiche (MF) 76

MECHANICS OF A CONED ROTATING NET

by Richard H. MacNeal

Prepared under Contract No. NAS 7-272 by
ASTRO RESEARCH CORPORATION
Santa Barbara, Calif.

for

MECHANICS OF A CONED ROTATING NET

By Richard H. MacNeal

Distribution of this report is provided in the interest of information exchange. Responsibility for the contents resides in the author or organization that prepared it.

Prepared under Contract No. NAS 7-272 by
ASTRO RESEARCH CORPORATION
Santa Barbara, Calif.

for

NATIONAL AERONAUTICS AND SPACE ADMINISTRATION

For sale by the Clearinghouse for Federal Scientific and Technical Information
Springfield, Virginia 22151 - Price \$3.00

ABSTRACT

27396

The deformations, stresses, and vibration modes of a rotating net in a hypersonic air stream are analyzed. Particular emphasis is placed on the "isotensoid" net of fiber circles that has the property that fiber stress is everywhere equal when the spinning net is flat.

Numerical solutions are obtained for the large motion static deformations and stresses in an axisymmetric hypersonic air stream including the effects of tip weights, hub radius, etc.

General expressions are written for the potential and kinetic energies for small perturbations from an axisymmetric state of equilibrium. These expressions are used to obtain numerical solutions for a variety of vibration problems including in-plane and out-of-plane vibrations of a flat net and the coupled vibrations of a statically deformed net. *Author*

TABLE OF CONTENTS

	<u>Page</u>
1. INTRODUCTION	1
2. NET GEOMETRY	3
3. STATIC AXISYMMETRIC DEFORMATION WITHOUT ELASTIC DISTORTION IN A HYPERSONIC STREAM	6
4. ENERGY EXPRESSIONS FOR SMALL MOTIONS FROM AN AXISYMMETRIC STATE OF EQUILIBRIUM	16
5. OUT-OF-PLANE VIBRATIONS OF A FLAT ROTATING ISOTENSOID NET. . . .	23
6. CRITICAL SPEED FOR MASS UNBALANCE OF A FLAT ISOTENSOID NET . . .	29
7. VIBRATIONS OF A CONED NET	34
REFERENCES	38
APPENDIX A: METHOD FOR OBTAINING NUMERICAL SOLUTIONS TO VIBRATION PROBLEMS	

LIST OF ILLUSTRATIONS

<u>Fig. No.</u>	<u>Page</u>
1. Portion of a Rotor Net	39
2. Isotenoid Net of Fiber Circles	39
3. Geometrical Parameters of Isotenoid Net	40
4. Forces Acting on the Net	40
5. Static Equilibrium of an Elemental Fiber Diamond	41
6. Rotating Net Vertical Deflection	42
7. Variation of Coning Angle With Mean Coning Angle, β_m	43
8. Variation of Fiber Stress With β_m	44
9. Effect of γ_{ot} on Local Coning Angle	45
10. Effect of γ_{ot} on Fiber Stress	46
11. Effect of ℓ_m/R on Fiber Stress	47
12. Variation of Drag Coefficient, C_D , With Mean Coning Angle, β_m	48
13. Displacement Components for Small Motions of an Axisymmetric Net	49
14. Elastic Distortion Without Rotation of a Fiber Diamond	50
15. Static Forces Acting on an Elemental Diamond	51
16. Out-Of-Plane Vibration of a Flat Isotenoid Net	52
17. Apparent In-Plane Mass of a Rotor Net When Excited From the Hub at One Cycle per Revolution in the Stationary System	53
18. Coned Net Vibration Frequency Summary	54
19. First Tangential Mode for Flat Net, $\bar{\omega} = 1.26$, $\beta_m = 0$, $E/\sigma_0 = 100$	55

LIST OF ILLUSTRATIONS
(Cont.)

<u>Fig. No.</u>	<u>Page</u>
20. First Flapping Mode, $\bar{\omega} = 0.92$, $\beta_m = 0.2$, $E/\sigma_o = 100$	56
21. First Flapping Mode, $\bar{\omega} = 0.96$, $\beta_m = 0.2$, $E/\sigma_o = 500$	57
22. First Tangential Mode, $\bar{\omega} = 1.22$, $\beta_m = 0.2$, $E/\sigma_o = 100$	58
23. First Tangential Mode, $\bar{\omega} = 1.65$, $\beta_m = 0.2$, $E/\sigma_o = 500$	59
24. First Flapping Mode, $\bar{\omega} = 0.67$, $\beta_m = 0.4$, $E/\sigma_o = 100$	60
25. First Tangential Mode, $\bar{\omega} = 1.15$, $\beta_m = 0.4$, $E/\sigma_o = 100$	61

L I S T O F S Y M B O L S

a	= radius of fiber circle for isotensoid net
A	= cross-sectional area of fibers
b	= hub radius
C	= capacity
C_D	= drag coefficient
D	= drag force developed by net
e	= voltage
E	= $V_e + V_s - T$ = Total energy
E	= Young's modulus
F_{n_a}	= aerodynamic force per unit area, normal to surface
F_r	= radial centrifugal force density
ℓ	= length of side of fiber diamond
ℓ_a	= effective length of aerodynamic surface of tip weights
ℓ_m	= m_t/m_o , tip weight parameter
L	= inductance
m	= mass per unit area of the net
m'	= mass per unit area of net when flat
m_o	= mass per unit area just inside the outer periphery when the net is flat
m_t	= tip mass per unit length when net is flat
n	= number of wavelengths around the circumference
N	= total number of fibers per radian
N_s	= meridional tensile force per unit width
N_θ	= circumferential tensile force per unit width
r	= distance to polar axis

L I S T O F S Y M B O L S

(Cont.)

r_o	=	value of r when net is flat
R	=	rotor radius when net is flat
s	=	distance along meridian
t	=	time, (tangential coordinate in Fig. 14 only)
T	=	fiber tension
T	=	kinetic energy
u_r	=	perturbation radial motion
u_s	=	perturbation motion in direction of meridian
u_z	=	perturbation motion parallel to axis
u_θ	=	circumferential perturbation motion
U	=	free stream velocity parallel to rotor axis
V_c	=	stored energy of capacitor
V_e	=	elastic strain energy
V_L	=	stored energy of inductor
V_s	=	energy due to static preload
w	=	perturbation motion normal to surface of net
β	=	coning angle
β_m	=	mean coning angle = $\rho U^2 / \Omega^2 R m_o$
γ	=	angle between fiber and line through the polar axis
γ_o	=	value of γ when net is flat
γ_{ot}	=	value of γ at the tip when net is flat
ϵ_s	}	components of membrane strain
ϵ_θ		
$\epsilon_{s\theta}$		

L I S T O F S Y M B O L S

(Cont.)

θ_s $\left. \begin{array}{l} \theta_\emptyset \\ \theta_w \end{array} \right\}$ components of rotation (assumed small)

ρ = free stream atmospheric density

ρ_f = density of fiber material

σ = fiber stress

σ_o = fiber stress of flat isotenoid disc

\emptyset = azimuth angle

ω = frequency, radians/sec

$\bar{\omega}$ = ω/Ω

Ω = rotational speed, radians/sec

subscript (b) refers to value at hub

subscript (t) refers to value at tip

(-) over quantity means quantity is non-dimensionalized according to Eqn. (3-15), or according to Eqns. (6-9) and (6-10)

MECHANICS OF A CONED ROTATING NET

1. INTRODUCTION

The present report represents a part of the effort expended during a recent investigation into the feasibility of employing rotating nets as atmospheric decelerators. In such applications a net would be constructed as a closely-woven fabric of high-strength fibers and would support aerodynamic load normal to its surface by means of centrifugal force. In general the rotor net is characterized by extremely low values of ballistic coefficient, $m/C_D A$, and low structural weight. Operation in both the hypersonic and subsonic phases of atmospheric entry is contemplated.

The subject of this report is the analysis of the deformations and stresses of a rotor net for the simplest and most elementary conditions excluding, for example, flight at an angle of incidence to the airstream. A high standard of mathematical rigor is maintained in order to provide a reliable basis for future investigations. Other aspects of the present rotor net investigation are reported in references 4 and 5.

The rotor net has certain features that tend to simplify the mathematical analysis of its motions. These include the absence of significant bending rigidity, rotational symmetry, and the ability to undergo some types of large deformation without appreciable elastic strain. On the other hand the analysis of the rotor net is complicated by the effects of rotation, particularly those that are identified as Coriolis and centrifugal stiffening effects.

In this report, the analysis of large static deformations due to axisymmetric air load is taken up first. The next topic is a general treatment of potential and kinetic energy for small motions from a state of equilibrium. The report concludes with a series of analyses of the vibrations of flat nets and nets that are coned up due to axisymmetric air load.

2. NET GEOMETRY

The nets that will be considered are constructed from two symmetrical sets of very slender fibers that intersect to form elemental diamonds as shown in Fig. 1. Such nets can be deformed from a plane into a smooth axisymmetric surface without appreciable elastic distortion. This property is particularly useful in aerodynamic applications where the maintenance of a smooth surface is important.

In general it will be assumed that the net is supported at its inner boundary by a rigid hub. In some instances concentrated weights will be located at the periphery of the net.

Special attention will be paid to the case in which the fibers of the net describe circles that pass through the axis of symmetry as shown in Fig. 2. It has been shown (Ref. 1) that the stress in the fibers of such a net is everywhere constant when the net is rotated to produce a radial centrifugal force distribution proportional to the mass density of the fibers. It will be of particular interest to determine whether, and to what extent, the constant-stress property of the rotating "isotenoid" net is maintained when the net is subjected to axisymmetric aerodynamic loading.

The isotenoid net of circular fibers has certain geometrical properties that will be used repeatedly in the work that follows. Consider an individual fiber circle shown in Fig. 3a. The angle that the fiber circle makes with a radial line is related to the distance from the polar axis by

$$\sin \gamma = \frac{r}{2a} \quad (2-1)$$

where a is the radius of the fiber circle.

The length of the side of an elemental diamond of the net, Fig. 3b, may be calculated by considering that the sum of the transverse diagonals at a fixed radius is equal to the circumference. Thus

$$2\pi r = 2\pi N \ell \sin \gamma \quad (2-2)$$

where N is the number of fibers per radian in both sets. Using Eqn. (2-1)

$$\ell = \frac{2a}{N} \quad (2-3)$$

so that the side lengths of all elemental diamonds in the isotenoid net are equal.

The mass per unit area of the isotenoid net is related to the properties of the fibers by

$$m' = \frac{\rho_f A N}{r \cos \gamma} = \frac{\rho_f A N}{a \sin 2\gamma} \quad (2-4)$$

where

ρ_f = density of fiber material

A = cross-sectional area of fibers

It is seen from Eqn. (2-4) that the mass density of the net becomes

very large near the axis ($r \rightarrow 0$) and near the periphery ($r \rightarrow 90^\circ$). Thus in practical applications the net will be terminated in a rigid hub near the axis and in a set of concentrated weights at the periphery.

3. STATIC AXISYMMETRIC DEFORMATION WITHOUT ELASTIC DISTORTION IN A HYPERSONIC STREAM

The problem considered here is the determination of the shape that an axisymmetric net will take when rotating about its axis and subjected to a hypersonic stream parallel to the axis. Stresses in the fibers of the net will also be computed.

Since the deformations that are contemplated are large, it will not be possible to use small motion theory. The complexity of the problem is, therefore, such that a digital computer is required to obtain numerical results.

The loads acting on the net are shown in Fig. 4. The net is subjected to a radial centrifugal force density per unit area

$$F_r = m\Omega^2 r \quad (3-1)$$

where

m = mass per unit area of the net

Ω = rotational speed rad/sec

r = distance to the axis of rotation

The aerodynamic load is computed using the Newtonian flow concept. The aerodynamic force per unit area normal to the surface of the net is

$$F_{n_a} = \rho U^2 \cos^2 \beta \quad (3-2)$$

where

ρ = free stream atmospheric density

U = velocity of the net parallel to the axis of rotation

β = local coning angle between the tangent to the net and a plane perpendicular to the axis of rotation.

The loads are equilibrated by the forces in the fibers of the net.

Let N_s be the internal tensile force per unit width of net directed along the intersection of the net with a radial plane and let N_θ be the internal tensile force per unit width of net directed along the intersection of the net with a circular cylinder. The equations for equilibrium of forces in a radial plane are

$$\frac{1}{r} \frac{\partial}{\partial r} (N_s r) - \frac{N_\theta}{r} + F_r = 0 \quad (3-3)$$

and

$$\frac{\partial \beta}{\partial r} = - \frac{N_\theta}{N_s} \frac{\tan \beta}{r} - \frac{F_{na} - F_r \sin \beta}{N_s \cos \beta} \quad (3-4)$$

The above equations are applicable to any axisymmetric shell in which bending moments are negligible, for example, a thin metal sheet. In the case of a net the force densities N_s and N_θ are not independent. They are related through the statics of an elementary fiber diamond as shown in Fig. 5. The relationship is

$$N_\theta = N_s \tan^2 \gamma \quad (3-5)$$

which may be used to eliminate N_θ from Eqns. (3-3) and (3-4). These equations become, using Eqns. (3-1) and (3-2)

$$\frac{\partial}{\partial r} (N_s r) - N_s \tan^2 \gamma + m\Omega^2 r^2 = 0 \quad (3-6)$$

and

$$\frac{\partial \beta}{\partial r} = - \tan^2 \gamma \frac{\tan \beta}{r} - \frac{\rho U^2 \cos^2 \beta - m\Omega^2 r \sin \beta}{N_s \cos \beta} \quad (3-7)$$

The angle γ appearing in these equations is not independent of the deformations of the net. Equation (2-2), which relates γ to the distance from the axis of revolution, is valid for any axisymmetrically deformed shape. Thus

$$\frac{\sin \gamma}{\sin \gamma_0} = \frac{r}{r_0} \quad (3-8)$$

where r_0 is the radius and γ_0 is the angle when the net is flat.

Likewise, for the slant length of the deformed diamond,

$$\frac{\Delta s}{\Delta r_0} = \frac{\cos \gamma}{\cos \gamma_0} \quad (3-9)$$

so that, replacing the small diamonds by infinitesimals

$$\frac{dr}{dr_0} = \cos \beta \frac{ds}{dr_0} = \frac{\cos \beta \cos \gamma}{\cos \gamma_0} \quad (3-10)$$

Equations (3-6), (3-7), (3-8) and (3-10) are a set of four differential equations in the dependent variables r , β , γ and N_s which will be integrated with respect to r_o . It should first, however, be noted that m , the mass per unit area, is not independent of the deformation since it varies inversely with the area of the elemental diamond. Thus

$$m = m' \cdot \frac{\sin 2\gamma_o}{\sin 2\gamma} \quad (3-11)$$

where m' , the mass per unit area when the net is flat, may be evaluated by means of Eqn. (2-4).

Three boundary conditions are required to complete the specification of the integration problem. One condition is that, at the inner edge of the net

$$r = b, \text{ at } r_o = b \quad (3-12)$$

The other two boundary conditions are applied at the outer edge of the net, $r_o = R$. It will be assumed that small tip weights with aerodynamic surfaces are attached to the periphery of the net. The equilibrium of aerodynamic and centrifugal forces on the tip weights requires that

$$\ell_a \rho U^2 \cos^2 \beta_t = m_t \Omega^2 r_t \sin \beta_t \quad (3-13)$$

where

$$\ell_a = \frac{S_a}{2\pi R} = \text{effective length of aerodynamic surface}$$

m_t = tip mass per unit length when the net is flat.

The load per unit length in the net at the rim is

$$N_{s_t} = F_r \cos \beta_t = \left\{ m_t \frac{R}{r_t} \right\} \Omega^2 r_t \cos \beta_t \quad (3-14)$$

Before indicating the method of solution, the equations describing the problem will be normalized and collected together. Let

$$\left. \begin{aligned} r &= \bar{r} R \\ r_o &= \bar{r}_o R \\ b &= \bar{b} R \\ r_t &= \bar{r}_t R \\ N_s &= \bar{N}_s \rho U^2 R \end{aligned} \right\} \quad (3-15)$$

Define the parameter

$$\beta_m = \frac{\rho U^2}{\Omega^2 R m_o} \quad (3-16)$$

where m_o is the mass per unit area just inside the outer periphery when the net is flat.

β_m is the coning angle that would result (at small coning) if mass density \times radius were constant.

The normalized equations of state are

$$\frac{\partial \bar{N}_s}{\partial \bar{r}} = \frac{\bar{N}_s}{\bar{r}} \left\{ \tan^2 \gamma - 1 \right\} - \frac{m_t}{m_o} \frac{\sin 2\gamma_o}{\sin 2\gamma} \frac{\bar{r}}{\beta_m} \quad (3-17)$$

$$\frac{\partial \beta}{\partial \bar{r}} = \frac{-\tan^2 \gamma \tan \beta}{\bar{r}} - \frac{1}{\bar{N}_s} \left\{ \cos \beta - \frac{m'}{m_o} \frac{\sin 2\gamma_o}{\sin 2\gamma} \frac{\bar{r} \tan \beta}{\beta_m} \right\} \quad (3-18)$$

$$\frac{d\bar{r}}{d\bar{r}_o} = \frac{\cos \beta \cos \gamma}{\cos \gamma_o} \quad (3-19)$$

$$\sin \gamma = \sin \gamma_o \frac{\bar{r}}{\bar{r}_o} \quad (3-20)$$

while the normalized boundary conditions are

$$\bar{r} = \bar{b} \quad \text{at} \quad \bar{r}_o = \bar{b} \quad (3-21)$$

$$\left. \begin{aligned} \frac{\sin \beta}{\cos^2 \beta} &= \frac{\ell_a}{\ell_m} \cdot \frac{\beta_m}{\bar{r}} \\ \bar{N}_s &= \frac{\ell_m}{R} \cdot \frac{\cos \beta}{\beta_m} \end{aligned} \right\} \quad \text{at} \quad \bar{r}_o = 1 \quad (3-22)$$

$$\left. \begin{aligned} \frac{\sin \beta}{\cos^2 \beta} &= \frac{\ell_a}{\ell_m} \cdot \frac{\beta_m}{\bar{r}} \\ \bar{N}_s &= \frac{\ell_m}{R} \cdot \frac{\cos \beta}{\beta_m} \end{aligned} \right\} \quad \text{at} \quad \bar{r}_o = 1 \quad (3-23)$$

where $\ell_m = m_t/m_o$ is the width of the strip of net near the periphery that has the same mass as the tip weights.

The parameters that describe the problem are

1. β_m , the "mean" coning angle
2. \bar{b} , the dimensionless hub radius
3. $\frac{\ell_m}{R}$, a parameter describing the size of the tip weights.
4. $\frac{\ell_a}{\ell_m}$, a parameter describing the proportion of tip weight area that is aerodynamically effective

5. $\frac{m'}{m_o}$ vs \bar{r}_o , the mass distribution of the flat net
6. γ_o vs \bar{r}_o , the spiral angle of the flat net

For the special case of an "isotenoid" net of circular fibers which is terminated at a radius smaller than the diameter of the fiber circles, the spiral angle at the tip will be

$$\gamma_{o_t} = \sin^{-1}\left(\frac{R}{2a}\right) \quad (3-24)$$

where $2a$ is the diameter of the fiber circle.

The spiral angle at other radii is given by

$$\gamma_o = \sin^{-1}\left\{\frac{r_o}{2a}\right\} = \sin^{-1}(\bar{r}_o \sin \gamma_{o_t}) \quad (3-25)$$

For such nets the mass distribution, as obtained from Eqn. (2-4) is

$$\frac{m'}{m_o} = \frac{\sin 2\gamma_{o_t}}{\sin 2\gamma_o} \quad (3-26)$$

Thus the mass distribution and spiral angle of nets with circular fiber patterns are both specified by γ_{o_t} , the spiral angle at the periphery of the net.

The differential equations are solved as a pseudo initial value problem by arbitrarily specifying a value of \bar{r} at $\bar{r}_o = 1$. Values of β and \bar{N}_s may then be obtained from Eqns. (3-22) and (3-23) to provide starting values for the step-by-step numerical integration of Eqns. (3-17)

to (3-20). Unless the correct value of \bar{r} at the tip has been selected it will be found, after integrating the equations of state, that the boundary condition at the hub, Eqn. (3-21), is not satisfied. Other trial values of \bar{r} at the tip are selected and solutions calculated until the error in the hub boundary condition is considered to be sufficiently small. Alternatively \bar{b} may be regarded as a variable parameter, so that every trial value of \bar{r} at the tip yields a correct solution for \bar{b} equal to the value of \bar{r}_0 at which $\bar{r} = \bar{r}_0$.

Once the normalized equations have been solved, the stress in the fibers of the net is obtained from

$$\sigma = \frac{T}{A} = \frac{N_s \ell \tan \gamma}{A} = \frac{N_s}{N_s} \rho U^2 R \ell \tan \gamma / A \quad (3-27)$$

For the special case of the isotenoid net of circles, it may be shown, Ref. 1, that the fiber stress for a flat disc is

$$\sigma_0 = 2a^2 \Omega^2 \rho_f \quad (3-28)$$

It is of interest to compare the actual fiber stress with σ_0 . If the actual net is also a net of fiber circles then it may be shown, after some manipulation, that

$$\frac{\sigma}{\sigma_0} = 2\bar{N}_s \beta_m \tan \gamma_{ot} \tan \gamma \quad (3-29)$$

where the basis of comparison between the actual net and the flat net is that they have the same angular velocity Ω .

The total drag force for the rotor net may be expressed in the form

$$D = \frac{1}{2} \rho U^2 \pi R^2 C_D \quad (3-30)$$

where C_D is the drag coefficient. The drag may be computed from the value of N_s at the hub

$$D = 2\pi b N_{s_b} \sin\beta_b \quad (3-31)$$

where β_b is the coning angle at $r = b$. Comparing Eqns. (3-31) with (3-30), and using the definitions of Eqn. (3-15)

$$C_D = 4\bar{b} \bar{N}_{s_b} \sin\beta_b \quad (3-32)$$

Representative numerical results are presented in Figs. 6 through 12. Figure 6 shows the shape that the rotor net assumes for three different values of the coning parameter, β_m . For low coning the net has a flared appearance, being flatter near the rim than it is near the hub. For high coning the net has a more nearly conical shape. These characteristics are seen more clearly in Fig. 7, which shows the local coning angle as a function of \bar{r}_o . The fiber stress is plotted in Fig. 8 where it is seen that large coning increases the variation of fiber stress with distance from the hub.

The fiber spiral angle at the rim, γ_{ot} , has a pronounced effect on the flare of the rotor net, Fig. 9, and also on fiber stress, Fig. 10. A low value of γ_{ot} decreases the flare but increases the variation of fiber stress with distance from the hub.

The effect of changes in tip weight on fiber stress is plotted in Fig. 11. For low coning a value of tip weight can be found that will produce a nearly uniform fiber stress. This result cannot be achieved for high coning. The effect of tip weight size on coning angle was found to be small. The effects of variations in the hub radius, \bar{b} , and the aerodynamic effectiveness of the tip weights, ℓ_a/ℓ_m , were also investigated and were found to be small.

The variation of drag coefficient with the coning parameter, β_m , is plotted in Fig. 12.

In the theory and calculations presented here it is assumed that all of the drag force is reacted at the hub. Thus in a condition of uniform deceleration during atmospheric reentry, the effects of axial inertia force on the net itself are neglected. If the coning angle and mass distribution were uniform over the surface of the net, these effects would be zero. Since the net is more dense near the hub and the rim than it is at points between, the major effect of inertia force on the net will be to increase the flare.

Another important assumption is that the flow through the pores of the net is negligibly small and does not alter the normal force coefficient predicted by Newtonian flow theory. It may be shown that the assumption is valid under hypersonic flow conditions provided that the porosity is not so large that shock waves form around individual fibers rather than standing off from the rotor net.

4. ENERGY EXPRESSIONS FOR SMALL MOTIONS FROM AN AXISYMMETRIC STATE OF EQUILIBRIUM

Small motion theory is valid for the solution of many of the practical problems that arise in connection with a rotating net decelerator, including vibrations, flutter, dynamic loads, flight stability, and control. Energy expressions based on small motion theory will be developed in this section for subsequent application to vibration problems.

It will be assumed that an initially flat net is deformed by air loads into a surface of revolution. Components of displacement from the deformed equilibrium shape are defined in Fig. 13. The coordinate system is assumed to rotate with the net. s is the distance along a meridian.

The components of membrane strain and rotation with respect to the rotating coordinate system, as obtained from general expressions in Ref. 2, are:

STRAINS:

$$\epsilon_s = \frac{\partial u_s}{\partial s} - w \frac{\partial \beta}{\partial s} \quad (4-1)$$

$$\epsilon_\theta = \frac{1}{r} \frac{\partial u_\theta}{\partial \theta} + \frac{u_s \cos \beta - w \sin \beta}{r} \quad (4-2)$$

$$\epsilon_{s\theta} = r \frac{\partial}{\partial s} \left\{ \frac{u_\theta}{r} \right\} + \frac{1}{r} \frac{\partial u_s}{\partial \theta} \quad (4-3)$$

ROTATIONS (Right Hand Rule):

$$\theta_s = \frac{1}{r} \frac{\partial w}{\partial \theta} + \frac{u_\theta}{r} \sin \beta \quad (4-4)$$

$$\theta_\theta = - \frac{\partial w}{\partial s} - u_s \frac{\partial \beta}{\partial s} \quad (4-5)$$

$$\theta_w = \frac{1}{2r} \left\{ \frac{\partial (ru_\theta)}{\partial s} - \frac{\partial u_s}{\partial \theta} \right\} \quad (4-6)$$

Three types of energy will be considered. These are

1. Elastic energy due to membrane strain
2. Potential energy due to work done against the static preloads that are present because of centrifugal forces and static air load.
3. Kinetic energy due to perturbation motions.

The expression for elastic energy due to membrane strain may be computed by reference to the geometrical configuration of an individual fiber diamond. Figure 14 shows the motions of three of the vertices of a fiber diamond due to membrane strain. Rotation about an axis normal to the plane of the diamond is restrained to be zero. The elastic strain energy of fiber (a) is

$$\begin{aligned} V_{e_a} &= \frac{1}{2} \frac{EA}{\ell} (\Delta u_a)^2 \\ &= \frac{1}{2} EA \ell \left\{ \epsilon_s \cos^2 \gamma + \epsilon_\theta \sin^2 \gamma + \epsilon_{s\theta} \sin \gamma \cos \gamma \right\}^2 \end{aligned} \quad (4-7)$$

while the elastic strain energy of fiber (b) is

$$\begin{aligned}
V_{e_b} &= \frac{1}{2} \frac{EA}{\ell} (\Delta u_b)^2 \\
&= \frac{1}{2} EA \ell \left\{ \epsilon_s \cos^2 \gamma + \epsilon_\emptyset \sin^2 \gamma - \epsilon_{s\emptyset} \sin \gamma \cos \gamma \right\}^2 \quad (4-8)
\end{aligned}$$

The strain energy per unit area is

$$\begin{aligned}
\delta V_e &= \frac{V_{e_a} + V_{e_b}}{2\ell^2 \sin \gamma \cos \gamma} = \frac{EA}{2\ell \sin \gamma \cos \gamma} \left\{ (\epsilon_s \cos^2 \gamma + \epsilon_\emptyset \sin^2 \gamma)^2 \right. \\
&\quad \left. + \epsilon_{s\emptyset}^2 \sin^2 \gamma \cos^2 \gamma \right\} \quad (4-9)
\end{aligned}$$

which also may be written

$$\delta V_e = \frac{EA \sin 2\gamma}{4\ell} \left\{ (\epsilon_s \cot \gamma + \epsilon_\emptyset \tan \gamma)^2 + \epsilon_{s\emptyset}^2 \right\} \quad (4-10)$$

It will be noted that this expression is quite different from that for an isotropic membrane. For $\gamma = \pi/4$, the effective Poisson's ratio is 1.0.

In order to obtain an expression for the potential energy due to work done against the static preload, consider an elemental diamond as a free body with the preload forces acting at the vertices, and compute the work done when the diamond is displaced. The forces at the vertices must remain fixed in magnitude and direction during such virtual displacements in order that they may continue to be in equilibrium with the applied (unperturbed) aerodynamic and centrifugal loads.

The static forces acting on an elemental diamond are shown in Fig. 15. For any distortion of the diamond the work done per unit area against these forces is

$$\delta V_s = - \left\{ \frac{2N_s \ell \sin \gamma (u_{s_2} - u_{s_1}) + 2N_s \ell \sin \gamma \tan \gamma (u_{\emptyset_4} - u_{\emptyset_3})}{4\ell^2 \sin \gamma \cos \gamma} \right\} \quad (4-11)$$

The distortions to be considered are the three rotations, θ_s , θ_\emptyset and θ_w , and a change in the spiral angle of the diamond, $\delta\gamma$. The distortions enter into δV_s raised to the second and higher powers. Since we are interested only in the second powers of the distortions, it can be shown that it is permissible to consider their effects separately.

Consider first a change in the spiral angle. Then

$$u_{s_2} - u_{s_1} = 2\ell \left\{ \cos(\gamma + \delta\gamma) - \cos\gamma \right\} \quad (4-12)$$

$$u_{\emptyset_4} - u_{\emptyset_3} = 2\ell \left\{ \sin(\gamma + \delta\gamma) - \sin\gamma \right\} \quad (4-13)$$

or, to second order in $\delta\gamma$

$$u_{s_2} - u_{s_1} = 2\ell \left\{ \cos\gamma \left(1 - \frac{1}{2}(\delta\gamma)^2\right) - \sin\gamma \delta\gamma - \cos\gamma \right\} \quad (4-14)$$

$$u_{\emptyset_4} - u_{\emptyset_3} = 2\ell \left\{ \sin\gamma \left(1 - \frac{1}{2}(\delta\gamma)^2\right) + \cos\gamma \delta\gamma - \sin\gamma \right\} \quad (4-15)$$

Retaining only the second order terms

$$u_{s_2} - u_{s_1} = -\ell \cos\gamma (\delta\gamma)^2 \quad (4-16)$$

$$u_{\emptyset_4} - u_{\emptyset_3} = -\ell \sin\gamma (\delta\gamma)^2 \quad (4-17)$$

and, upon substituting into Eqn. (4-11)

$$\delta V_s = \frac{1}{2} N_s \sec^2 \gamma (\delta \gamma)^2 \quad (4-18)$$

It is desired to express $\delta \gamma$ in terms of the cartesian strains ϵ_s and ϵ_\emptyset . From the first order terms in Eqns. (4-14) and (4-15)

$$\epsilon_s = \frac{u_{s2} - u_{s1}}{2l \cos \gamma} = -\tan \gamma \cdot \delta \gamma \quad (4-19)$$

$$\epsilon_\emptyset = \frac{u_{\emptyset 4} - u_{\emptyset 3}}{2l \sin \gamma} = \cot \gamma \cdot \delta \gamma \quad (4-20)$$

Thus as long as elastic distortion is neglected there are two alternative expressions for $\delta \gamma$. The above pair of equations may be (arbitrarily) combined to give

$$\delta \gamma = \frac{1}{2} (-\epsilon_s \cot \gamma + \epsilon_\emptyset \tan \gamma) \quad (4-21)$$

and, substituting into Eqn. (4-18)

$$\delta V_s = \frac{1}{8} N_s \sec^2 \gamma (\epsilon_s \cot \gamma - \epsilon_\emptyset \tan \gamma)^2 \quad (4-22)$$

Note the symmetrical manner in which ϵ_s and ϵ_\emptyset enter Eqns. (4-22) and (4-10). No other reason is advanced, at present, for the arbitrary choice in Eqn. (4-21).

Proceeding now to the effects of the rotations (considered independently)

$$u_{s_2} - u_{s_1} = 2l \cos \gamma (\cos \theta_w - 1) + 2 \cos \gamma (\cos \theta_\emptyset - 1) \quad (4-23)$$

$$u_{\emptyset_4} - u_{\emptyset_3} = 2l \sin \gamma (\cos \theta_w - 1) + 2 \cos \gamma (\cos \theta_s - 1) \quad (4-24)$$

or, to second order in the distortions,

$$u_{s_2} - u_{s_1} = -l \cos \gamma (\theta_w^2 + \theta_\emptyset^2) \quad (4-25)$$

$$u_{\emptyset_4} - u_{\emptyset_3} = -l \sin \gamma (\theta_w^2 + \theta_s^2) \quad (4-26)$$

Upon substituting into Eqn. (4-11) and adding to the previous result for the spiral angle

$$\delta V_s = \frac{1}{2} N_s \left\{ \frac{1}{4} \sec^2 \gamma (\epsilon_s \cot \gamma - \epsilon_\emptyset \tan \gamma)^2 + \sec^2 \gamma \theta_w^2 + \theta_\emptyset^2 + \tan^2 \gamma \theta_s^2 \right\} \quad (4-27)$$

The expression for the kinetic energy density, omitting constant and first order terms is

$$\delta T = \frac{1}{2} m \left\{ (\dot{u}_r - u_\emptyset \Omega)^2 + (\dot{u}_\emptyset + u_r \Omega)^2 + \dot{u}_z^2 \right\} \quad (4-28)$$

where

$$u_r = u_s \cos \beta - w \sin \beta \quad (4-29)$$

is the radial component of displacement and

$$u_z = u_s \sin\beta + w \cos\beta \quad (4-30)$$

is the vertical component of displacement.

In terms of u_\emptyset , u_s , and w , Eqn. (4-28) is

$$\begin{aligned} \delta T = \frac{1}{2} m \left[\dot{u}_s^2 + \dot{u}_\emptyset^2 + \dot{w}^2 + 2\Omega \left\{ \cos\beta (\dot{u}_\emptyset u_s - \dot{u}_s u_\emptyset) + \sin\beta (\dot{w} u_\emptyset - \dot{u}_\emptyset w) \right\} \right. \\ \left. + \Omega^2 \left\{ u_\emptyset^2 + (u_s \cos\beta - w \sin\beta)^2 \right\} \right] \quad (4-31) \end{aligned}$$

The first three terms are ordinary inertia terms. The terms proportional to Ω are related to Coriolis forces while the terms proportional to Ω^2 may be regarded as a negative stiffness effect of centrifugal force. The positive stiffening effect of centrifugal force has been included in the calculation of the work done against static preload.

The total energy density of the net is

$$\delta E = \delta V_e + \delta V_s - \delta T \quad (4-32)$$

δV_e and δV_s are obtained from Eqns. (4-10) and (4-27) respectively. Expressions for the strains and rotations in terms of displacements, Eqns. (1-6), will be inserted into δV_e and δV_s as needed in the applications that follow.

5. OUT-OF-PLANE VIBRATIONS OF A FLAT ROTATING ISOTENSOID NET

As a simple example which results in a closed-form solution, the out-of-plane vibration modes of an isotensoid net of fiber circles will be computed. This example is the limiting case for small coning and will yield information that is valuable for the estimation of the response to dynamic loads and for the determination of the stability and control characteristics of a vehicle employing a rotor net decelerator.

For a flat net the in-plane motions, u_s and u_θ , do not couple with the out-of-plane motion, w . The appropriate energy expressions, derived from the work of the preceding section, are

$$\begin{aligned}\delta V_s &= \frac{1}{2} N_s (\theta_\theta^2 + \tan^2 \gamma \theta_s^2) \\ &= \frac{1}{2} N_s \left[\left\{ \frac{\partial w}{\partial s} \right\}^2 + \frac{\tan^2 \gamma}{r^2} \left\{ \frac{\partial w}{\partial \theta} \right\}^2 \right]\end{aligned}\quad (5-1)$$

and

$$\delta T = \frac{1}{2} m \dot{w}^2 \quad (5-2)$$

The total energy of the net

$$\begin{aligned}E &= \int_b^R \int_0^{2\pi} (\delta V_s - \delta T) r dr d\theta = \frac{1}{2} \int_b^R \int_0^{2\pi} \left\{ N_s \left[\left\{ \frac{\partial w}{\partial s} \right\}^2 + \frac{\tan^2 \gamma}{r^2} \left\{ \frac{\partial w}{\partial \theta} \right\}^2 \right] \right. \\ &\quad \left. - m \dot{w}^2 \right\} r dr d\theta\end{aligned}\quad (5-3)$$

Because of the polar symmetry of the net, the deflection of the net in any vibration mode must be a sinusoidal function of θ . Therefore let

$$w = w_n \cos(n\theta + \omega_n t) \quad (5-4)$$

which represents a wave traveling in the negative θ direction with velocity equal to ω_n/n radians/sec. A superposition of this wave with a similar wave traveling in the forward direction yields a mode shape with nodal lines along meridians.

Differentiate Eqn. (5-4) to obtain

$$\frac{\partial w}{\partial \theta} = -w_n n \sin(n\theta + \omega_n t) \quad (5-5)$$

$$\dot{w} = \frac{\partial w}{\partial t} = -w_n \omega_n \sin(n\theta + \omega_n t) \quad (5-6)$$

so that, substituting into Eqn. (5-3) and integrating with respect to θ

$$E = \frac{\pi}{2} \int_b^R \left\{ N_s r \left[\left\{ \frac{\partial w_n}{\partial r} \right\}^2 + \frac{n^2}{r^2} \tan^2 \gamma w_n^2 \right] - m r \omega_n^2 w_n^2 \right\} dr \quad (5-7)$$

For a net of fiber circles, Eqns. (2-3), (2-4), (3-27) and (3-8) may be used to put Eqn. (5-7) into the following form

$$E = \frac{\pi}{2} \Omega^2 \rho_f A N \int_b^R \left\{ 2a^2 \cos \gamma \left[\left\{ \frac{\partial w_n}{\partial r} \right\}^2 + \frac{n^2}{4a^2} \sec^2 \gamma w_n^2 \right] - \frac{\omega_n^2}{\cos \gamma} w_n^2 \right\} dr \quad (5-8)$$

where

$$\bar{\omega}_n = \frac{\omega_n}{\Omega}$$

It is convenient to change the variable of integration from r to γ . Then by virtue of Eqn. (2-1)

$$dr = 2a \cos \gamma \, d\gamma \quad (5-9)$$

and

$$\frac{\partial w_n}{\partial r} = \frac{1}{2a \cos \gamma} \cdot \frac{dw_n}{d\gamma} \quad (5-10)$$

Eqn. (5-8) becomes

$$E = \pi a \Omega^2 \rho_f A N \int_{\gamma_b}^{\gamma_t} \left\{ \frac{1}{2} \left[\left\{ \frac{dw_n}{d\gamma} \right\}^2 + n^2 w_n^2 \right] - \bar{\omega}_n^2 w_n^2 \right\} d\gamma \quad (5-11)$$

This problem of minimizing E may be transformed into a differential equation by means of the Euler equation

$$\frac{\partial E}{\partial w_n} - \frac{d}{d\gamma} \left\{ \frac{\partial E}{\partial w_n'} \right\} = 0 \quad (5-12)$$

where

$$w_n' = \frac{dw_n}{d\gamma} \quad (5-13)$$

The differential equation is

$$\frac{1}{2} \frac{d^2 w_n}{d\gamma^2} + \left\{ \bar{\omega}_n^2 - \frac{n^2}{2} \right\} w_n = 0 \quad (5-14)$$

which is an ordinary differential equation with constant coefficients.

Equation (5-14) will be solved with boundary conditions corresponding to a full net with no tip weight ($\gamma_t = \frac{\pi}{2}$) and a rigid restraint at the hub. Thus

$$w_n = 0 \quad \text{at} \quad \gamma = \gamma_b$$

$$\frac{dw_n}{d\gamma} = 0 \quad \text{at} \quad \gamma = \frac{\pi}{2}$$

The solutions of Eqn. (5-14) that satisfy the above boundary conditions are

$$w_n = \sin \left[m \frac{\pi}{2} \left(\frac{\gamma - \gamma_b}{\frac{\pi}{2} - \gamma_b} \right) \right] \quad (5-15)$$

where m is any odd integer.

Substitute this result into Eqn. (5-14) to obtain the normalized frequency of vibration

$$\bar{\omega}_n = \frac{1}{\sqrt{2}} \left[n^2 + \frac{m^2}{\left\{ 1 - \frac{2\gamma_b}{\pi} \right\}^2} \right]^{1/2} \quad (5-16)$$

cycles per revolution.

The above results may be used to estimate the dynamic response of the rotor. In steady lifting flight wherein the velocity vector is not parallel to the axis of revolution, the aerodynamic loads will not be axisymmetric. The loads will present a pattern that varies over the surface of the rotor disc but does not change with time as viewed from a non-

• rotating coordinate system. Thus, in a coordinate system that rotates with the rotor disc, the applied loads appear as a wave that travels opposite to the direction of rotation with angular velocity Ω . The applied load distribution can, therefore, be represented as a series of harmonic terms with the following form

$$F_{n_a} = \sum_{n=0}^{\infty} f_n(r) \cos(n\theta + n\Omega t + \alpha_n) \quad (5-17)$$

where $f_n(r)$ is a radial distribution function and α_n is a phase angle.

By comparing Eqns. (5-4) and (5-17), it is seen that a condition of resonance between the vibration modes of the rotor and the harmonic distribution of the applied load occurs when $\bar{\omega}_n = n$. Now m in Eqn. (5-16) can take on all odd-integral values so that, if $\gamma_b = 0$, resonances will occur for $n = 1, 3, 5, 7 \dots$. If γ_b is small, near resonances will occur for the same harmonics. For $\frac{2\gamma_b}{\pi} \ll 1$ and $n = m$ Eqn. (5-16) is approximated by

$$\begin{aligned} \bar{\omega}_n &= n \left\{ 1 + \frac{\gamma_b}{\pi} \right\} \\ &\approx n \left\{ 1 + \frac{b}{\pi R} \right\} \end{aligned} \quad (5-18)$$

It is concluded that the hub radius should be reasonably large, at least 5% of rotor radius, in order to prevent high dynamic amplification of harmonic air loads. The first harmonic ($n = 1$) air loads produce moments on the hub that must be balanced by a control mechanism in order to maintain trimmed lifting flight. The magnitude of the hub radius has therefore an important effect on the flight dynamics of the vehicle as a whole.

The mode shape for $n = m = 1$ and $b/R = .2$ is plotted versus radius in Fig. 16 where it is seen that the deviation from a straight line is very small.

6. CRITICAL SPEED FOR MASS UNBALANCE OF A FLAT ISOTENSOID NET

The usual definition for the critical speed of a rotating device is the lowest speed at which the frequency of a vibration mode, as viewed in the non-rotating system, is just equal to the speed of rotation. At the critical speed a small amount of rotating mass unbalance will resonate the vibration mode and cause high amplitude of response. As viewed in the rotating system, the frequency of vibration is zero at the critical speed. The unbalance force acts radially and can be represented by

$$F_r = \sum_{n=1}^{\infty} g_n(r) \cos(n\theta + \alpha_n) \quad (6-1)$$

where $g_n(r)$ is a radial distribution function and α_n is a phase angle. Only the term for $n = 1$ has an external resultant on the hub and it is for this term that the critical speed condition will be analyzed.

It will be assumed, for simplicity, that the net is flat. Under these conditions the in-plane motions do not couple with the out-of-plane motions. The relevant non-zero terms in the energy expressions of Section 4 are

$$\delta V_e = \frac{EA \sin 2\gamma}{4\ell} \left\{ (\epsilon_s \cot \gamma + \epsilon_\theta \tan \gamma)^2 + \epsilon_{s\theta}^2 \right\} \quad (6-2)$$

$$\delta V_s = \frac{1}{2} N_s \left\{ \frac{1}{4} \sec^2 \gamma (\epsilon_s \cot \gamma - \epsilon_\theta \tan \gamma)^2 + \sec^2 \gamma \theta_w^2 \right\} \quad (6-3)$$

$$\delta T = \frac{1}{2} m \Omega^2 (u_\theta^2 + u_s^2) \quad (6-4)$$

The appropriate expressions for strains and rotations are

$$\epsilon_s = \frac{\partial u_s}{\partial r} \quad (6-5)$$

$$\epsilon_\theta = \frac{1}{r} \frac{\partial u_\theta}{\partial \theta} + \frac{u_s}{r} \quad (6-6)$$

$$\epsilon_{s\theta} = r \frac{\partial}{\partial r} \left\{ \frac{u_\theta}{r} \right\} + \frac{1}{r} \frac{\partial u_s}{\partial \theta} \quad (6-7)$$

$$\theta_w = \frac{1}{2r} \left\{ \frac{\partial(ru_\theta)}{\partial r} - \frac{\partial u_s}{\partial \theta} \right\} \quad (6-8)$$

Due to the polar symmetry of the net and the choice of $n = 1$, let

$$u_s = \bar{u}_s \cos \theta \quad (6-9)$$

$$u_\theta = \bar{u}_\theta \sin \theta \quad (6-10)$$

Then

$$\epsilon_s = \frac{\partial \bar{u}_s}{\partial r} \cos \theta \quad (6-11)$$

$$\epsilon_\theta = \left\{ \frac{\bar{u}_\theta}{r} + \frac{\bar{u}_s}{r} \right\} \cos \theta \quad (6-12)$$

$$\epsilon_{s\theta} = \left\{ \frac{\partial \bar{u}_\theta}{\partial r} - \frac{\bar{u}_\theta}{r} - \frac{\bar{u}_s}{r} \right\} \sin \theta \quad (6-13)$$

$$\theta_w = \frac{1}{2} \left\{ \frac{\partial \bar{u}_\theta}{\partial r} + \frac{\bar{u}_\theta}{r} + \frac{\bar{u}_s}{r} \right\} \sin \theta \quad (6-14)$$

Upon substituting these expressions into Eqns. (6-2), (6-3) and (6-4) and integrating over the surface of the rotor

$$V_e = \int_b^R \frac{\pi}{4} \frac{EA \sin 2\gamma}{r} \left[\left\{ \frac{\partial \bar{u}_s}{\partial r} \cot \gamma + (\bar{u}_s + \bar{u}_\emptyset) \frac{\tan \gamma}{r} \right\}^2 + \left\{ \frac{\bar{u}_s + \bar{u}_\emptyset}{r} - \frac{\partial \bar{u}_\emptyset}{\partial r} \right\}^2 \right] r dr \quad (6-15)$$

$$V_s = \int_b^R \frac{\pi}{8} \frac{N_s}{\cos \gamma} \left[\left\{ \frac{\partial \bar{u}_s}{\partial r} \cot \gamma - (\bar{u}_s + \bar{u}_\emptyset) \frac{\tan \gamma}{r} \right\}^2 + \left\{ \frac{\bar{u}_s + \bar{u}_\emptyset}{r} + \frac{\partial \bar{u}_\emptyset}{\partial r} \right\}^2 \right] r dr \quad (6-16)$$

$$T = \int_b^R \frac{\pi}{2} m \Omega^2 (\bar{u}_s^2 + \bar{u}_\emptyset^2) r dr \quad (6-17)$$

For the special case of an isotensoid net of fiber circles, the coefficients appearing in these expressions are related by the fiber geometry such that

$$\begin{aligned} \bar{V}_e &= \frac{V_e}{\frac{\pi}{2} \Omega^2 m_o R} \\ &= \frac{E}{\sigma_o} \int_b^R \cos \gamma_t \cos \gamma \frac{r^2}{2} \left[\left\{ \frac{\partial \bar{u}_s}{\partial r} \cot \gamma + (\bar{u}_s + \bar{u}_\emptyset) \frac{\tan \gamma}{r} \right\}^2 + \left\{ \frac{\bar{u}_s + \bar{u}_\emptyset}{r} - \frac{\partial \bar{u}_\emptyset}{\partial r} \right\}^2 \right] dr \end{aligned} \quad (6-18)$$

$$\begin{aligned} \bar{V}_s &= \frac{V_s}{\frac{\pi}{2} \Omega^2 m_o R} \\ &= \int_b^R \frac{\cos \gamma_t}{\cos \gamma} \frac{a^2}{2} \left[\left\{ \frac{\partial \bar{u}_s}{\partial r} \cot \gamma - (\bar{u}_s + \bar{u}_\emptyset) \frac{\tan \gamma}{r} \right\}^2 + \left\{ \frac{\bar{u}_s + \bar{u}_\emptyset}{r} + \frac{\partial \bar{u}_\emptyset}{\partial r} \right\}^2 \right] dr \end{aligned} \quad (6-19)$$

$$\begin{aligned}\bar{T} &= \frac{T}{\frac{\pi}{2} \Omega^2 m_o R} \\ &= \int_b^R \frac{\cos \gamma_t}{\cos \gamma} \left\{ \bar{u}_s^2 + \bar{u}_\emptyset^2 \right\} dr\end{aligned}\quad (6-20)$$

It is assumed that the periphery of the net is weighted so that the static stress in the net is everywhere equal to σ_o , the stress for a set of full fiber circles. The required value of the tip weight parameter is

$$\ell_t = \frac{2a^2}{R} \cos^2 \gamma_t \quad (6-21)$$

Equations (6-18), (6-19) and (6-20), together with the boundary conditions at the hub and rim of the net, are a sufficient mathematical description of the problem to be solved. Appendix A describes a numerical method for obtaining solutions that accepts input information essentially in the form of the above energy expressions.

The particular physical situation for which solutions have been obtained is one in which an unbalanced force is applied to the net at a rigid hub. The ratio of the applied force to the resulting motion of the hub is proportional to the apparent mass of the rotor as viewed from the non-rotating coordinate system. This result is shown in Fig. 7 where the ratio of the apparent mass to the actual mass is plotted as a function of σ_o/E and the hub radius. In the case of an unrestrained vehicle with a rigid fuselage the critical value of σ_o/E occurs when the sum of the apparent mass of the rotor and the mass of the fuselage equals zero.

For example if the fuselage mass is two times the rotor mass, the critical value of σ_o/E is about 0.75. The resulting critical rotor speed may be obtained with the aid of Eqn. (3-28).

It will be observed that the critical value of σ_o/E exceeds 0.5 in all cases. Thus, with the exception of extremely elastic materials that can withstand strains of this magnitude, critical speeds for mass unbalance will be well above the operating rotor speed.

7. VIBRATIONS OF A CONED NET

The full generality of the equations derived in section 4 is required for the calculation of the vibration modes of a rotor net that is deformed by the action of steady axisymmetric air loads.

Let the motions of the net be described by an n^{th} harmonic backward traveling wave

$$w = w_n \cos(n\theta + \bar{\omega}_n \Omega t) + w_n^* \sin(n\theta + \bar{\omega}_n \Omega t) \quad (7-1)$$

$$u_s = u_{s_n} \cos(n\theta + \bar{\omega}_n \Omega t) + u_{s_n}^* \sin(n\theta + \bar{\omega}_n \Omega t) \quad (7-2)$$

$$u_\theta = u_{\theta_n} \sin(n\theta + \bar{\omega}_n \Omega t) - u_{\theta_n}^* \cos(n\theta + \bar{\omega}_n \Omega t) \quad (7-3)$$

The starred terms are included in view of the possibility that the phase angles between the three components of motion may not be exactly as indicated by the unstarred terms. However, it is easily shown by substitution into the general energy expressions that all energy terms proportional to the product of starred and unstarred components vanish identically. Therefore the starred and unstarred components are uncoupled and the phase relationships between the components of motion are those indicated for the unstarred components.

For motions of the above form the components of strain and rotation, Eqns. (4-1) to (4-6), become:

$$\epsilon_s = \left\{ \frac{\partial u_{s_n}}{\partial s} - \beta' w_n \right\} \cos(n\theta + \bar{\omega}_n \Omega t) \quad (7-4)$$

$$\epsilon_\theta = \left\{ \frac{n}{r} u_{\theta_n} + \frac{1}{r} (u_{s_n} \cos \beta - w_n \sin \beta) \right\} \cos(n\theta + \bar{\omega}_n \Omega t) \quad (7-5)$$

$$\epsilon_{s\theta} = \left\{ \frac{\partial u_{\theta_n}}{\partial s} - \frac{1}{r} (u_{\theta_n} \cos \beta + n u_{s_n}) \right\} \sin(n\theta + \bar{\omega}_n \Omega t) \quad (7-6)$$

$$\theta_s = \frac{1}{r} (u_{\theta_n} \sin \beta - n w_n) \sin(n\theta + \bar{\omega}_n \Omega t) \quad (7-7)$$

$$\theta_\theta = \left\{ \frac{\partial w_n}{\partial s} + \beta' u_{s_n} \right\} \cos(n\theta + \bar{\omega}_n \Omega t) \quad (7-8)$$

$$\theta_w = \frac{1}{2} \left\{ \frac{\partial u_{\theta_n}}{\partial s} + \frac{1}{r} (u_{\theta_n} \cos \beta + n u_{s_n}) \right\} \sin(n\theta + \bar{\omega}_n \Omega t) \quad (7-9)$$

where the abbreviation, $\beta' = \frac{\partial \beta}{\partial s}$, has been used.

The expressions for energy obtained by substituting the strains and rotations into Eqns. (4-10), (4-27), and (4-31) and integrating over the surface of the net will not be written here in view of the straight forwardness of the process and the complexity of the result.

Solutions have been obtained by the method described in Appendix A (with greater complication due to the proliferation of terms) for the case of an isotenoid net of fiber circles. Input data regarding the equilibrium shape and state of stress in the net have been taken from the results presented in section 3. The cases considered are the $n = 1$ modes with a rigid hub and the following parameters held fixed:

$$r_{ot} = 70^\circ; \quad \frac{b}{R} = 0.1; \quad \frac{\ell_m}{R} = .05; \quad \frac{\ell_a}{\ell_m} = 1.0$$

The frequencies of the three lowest modes are plotted in Fig. 18 as a function of the coning parameter, β_m . The following significant facts will be observed

1. The frequencies of modes identified as flapping modes (primarily out-of-plane motion) are nearly independent of the elastic modulus of the net material, whereas the frequency of the mode identified as the first tangential mode is strongly dependent on the modulus of the net material.
2. The frequencies of all modes decrease with increased coning. The frequency of the first flapping mode crosses the one/rev. line which has profound significance for the stability and control characteristics of a vehicle employing a rotor-net decelerator. Simplified analyses (see Ref. 3) usually yield the result that the frequency of the lowest flapping mode increases with increased coning.
3. The amount by which the frequency of the first tangential mode exceeds one cycle per revolution is roughly proportional to $\sqrt{E/\sigma_0}$.

The uncoupled mode shape for the first tangential mode is shown in Fig. 19. Large shear strain is indicated near the hub due to the small spiral angle, γ , of the fibers in this region. An increase in the spiral angle at the hub would probably result in a significant increase in the frequency of this mode.

Coupled mode shapes are shown in Figs. 20 to 25. The most surprising aspect of these results is that the sign of u_t in the first flapping mode

is opposite to that expected if the net were moving essentially as a rigid body. The only term that is capable of producing this unexpected result is the one that is proportional to β' in the expression for meridional strain, (Eqn. (7-4)). The effect of this term is that, due to the curvature of the net and the rigid kinematics of its diamond elements, a deflection in the direction of the outward normal to the surface tends to produce a contraction in the circumferential direction.

Figures 20 to 25 also indicate that the degree of coupling increases with increasing β_m and decreasing E/σ_0 . The latter result is expected in view of the proximity relationships between frequencies shown in Fig. 18.

A major conclusion from the results of this section is that both the lowest flapping mode and the lowest tangential mode should be included in a realistic analysis of the stability and control of a vehicle employing a rotor net decelerator. This becomes apparent when it is realized that the frequency of vibration in the stationary coordinate system is equal to the frequency of vibration in the rotating system minus the rotor speed so that both modes have low frequencies in the stationary system. Should the first tangential mode prove to have an adverse affect on stability, its frequency can be raised by increasing the spiral angle of the net near the hub.

REFERENCES

1. A. C. Kyser, "The Uniform Stress Spinning Filamentary Disc".
Report ARC-R-150, Astro Research Corporation, May, 1964.
2. A. E. H. Love, "A Treatise on the Mathematical Theory of Elasticity".
pp. 54-55, Dover Publications, N.Y., 1944.
3. R. H. MacNeal, "Elastic Circuit Analogies for Elastic Structures".
John Wiley & Sons, N.Y., 1962.
4. Final summary report under contract NAS7-272
5. Report on Flight Dynamics under contract NAS7-272

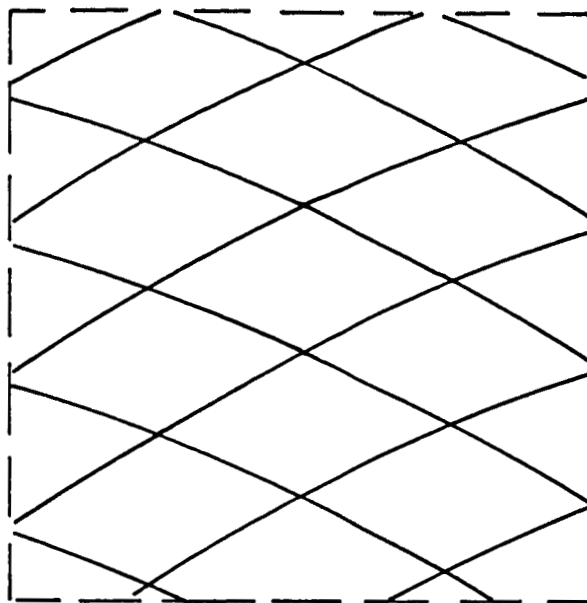


FIG. 1. Portion of Rotor Net

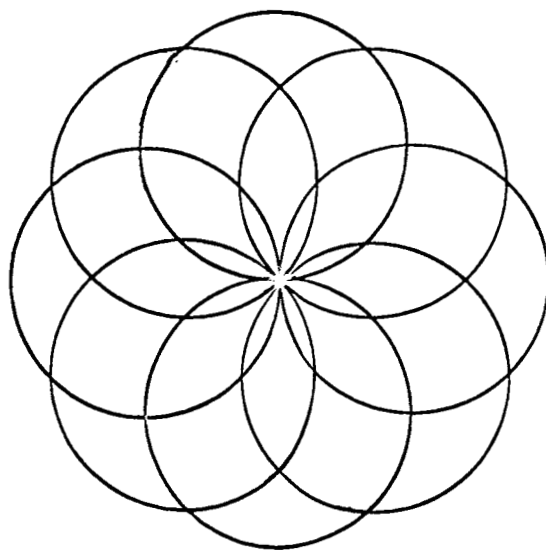
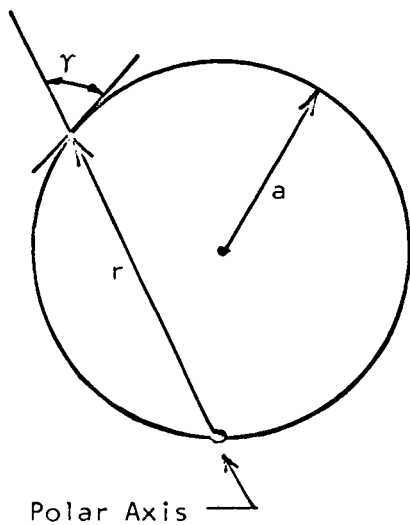
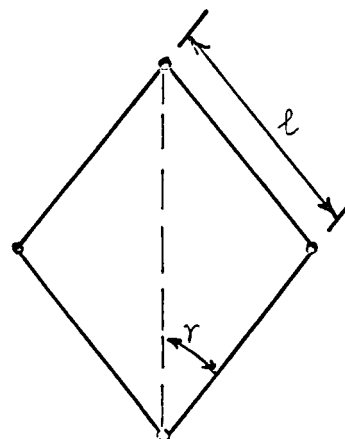


FIG. 2. Isotensoid Net of Fiber Circles



(a) Fiber Circle



(b) Elemental Fiber Diamond

FIG. 3. Geometrical Parameters of Isotenoid Net

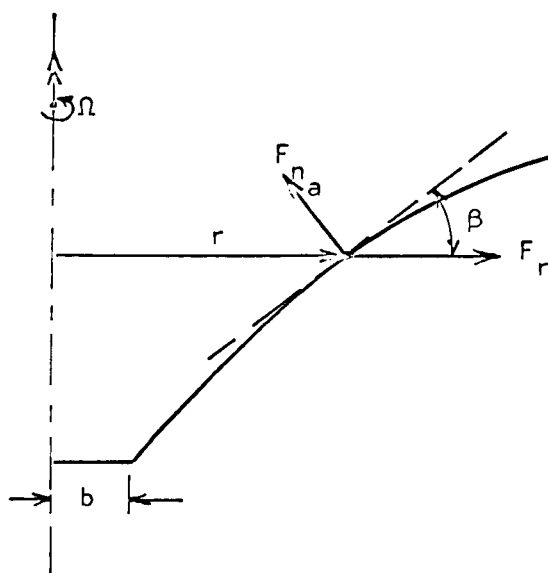


FIG. 4. Forces Acting on the Net

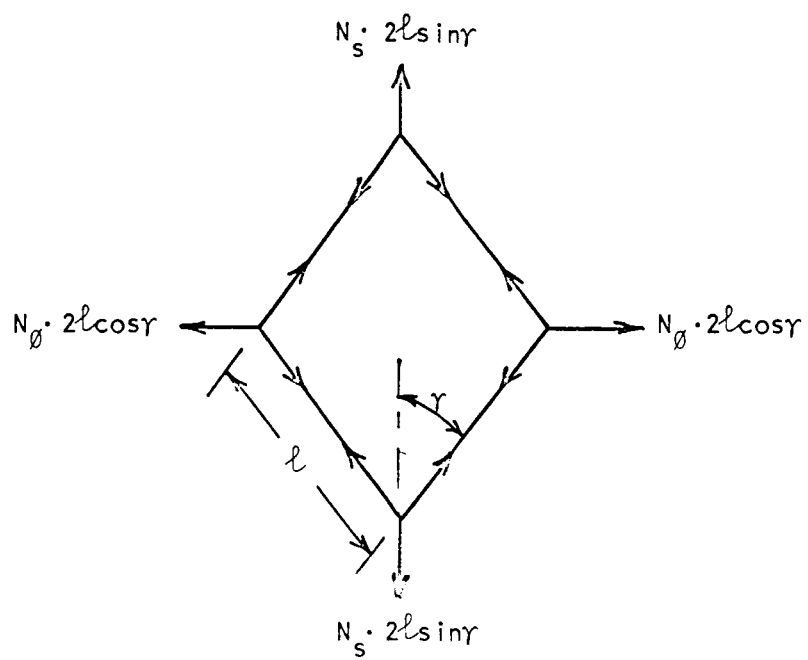


FIG. 5. Static Equilibrium of an Elemental Fiber Diamond

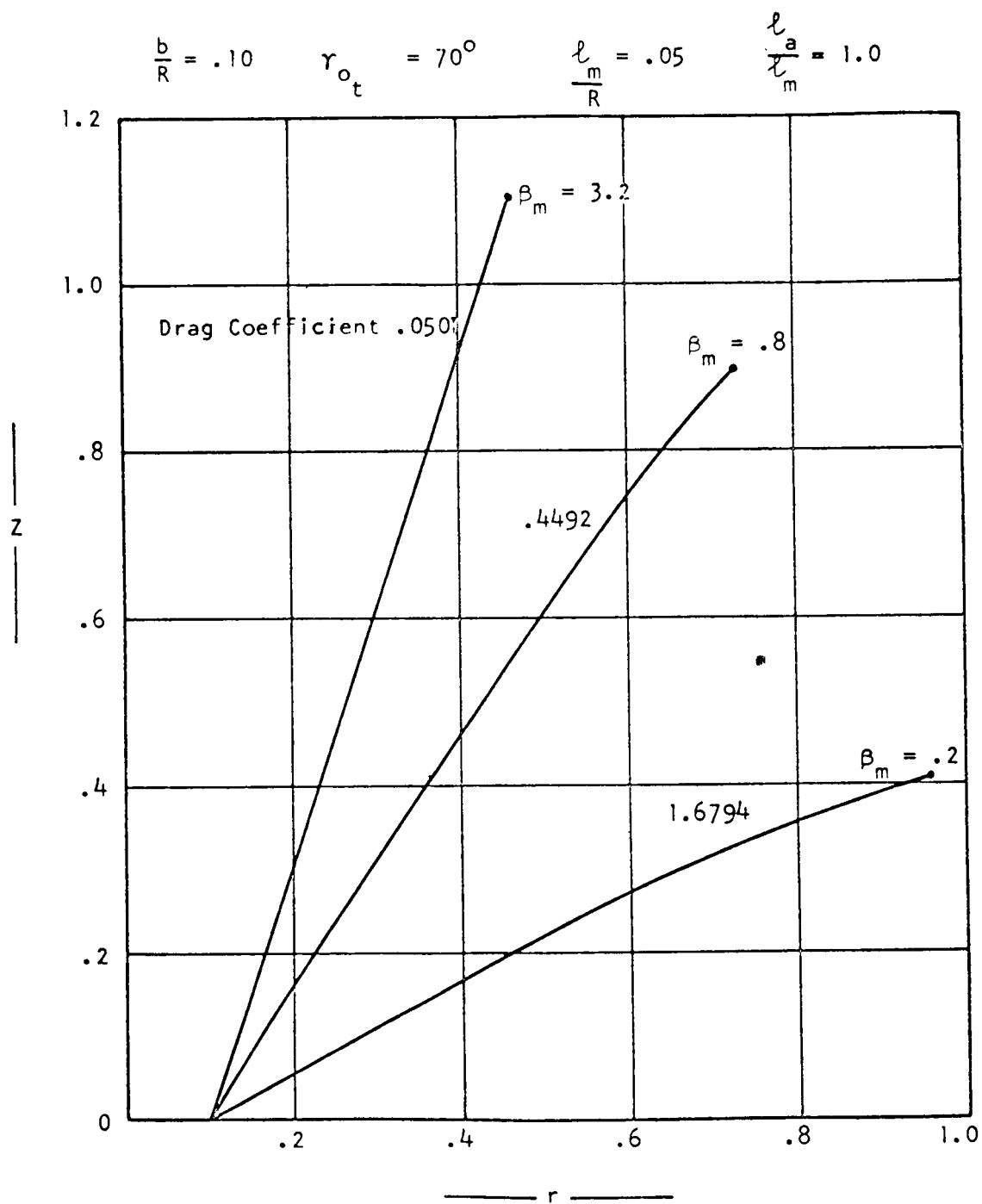


FIG. 6. ROTATING NET VERTICAL DEFLECTION

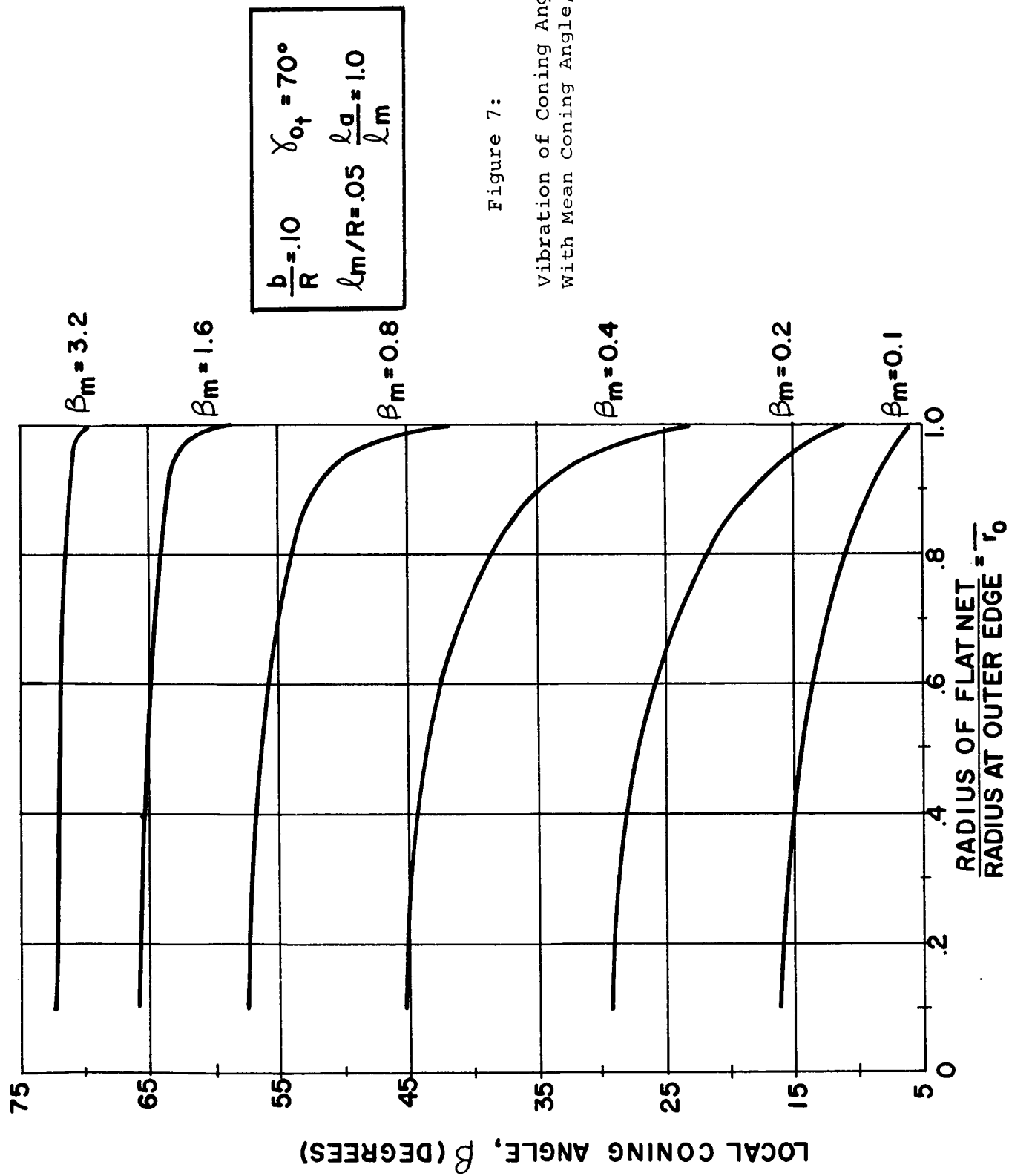
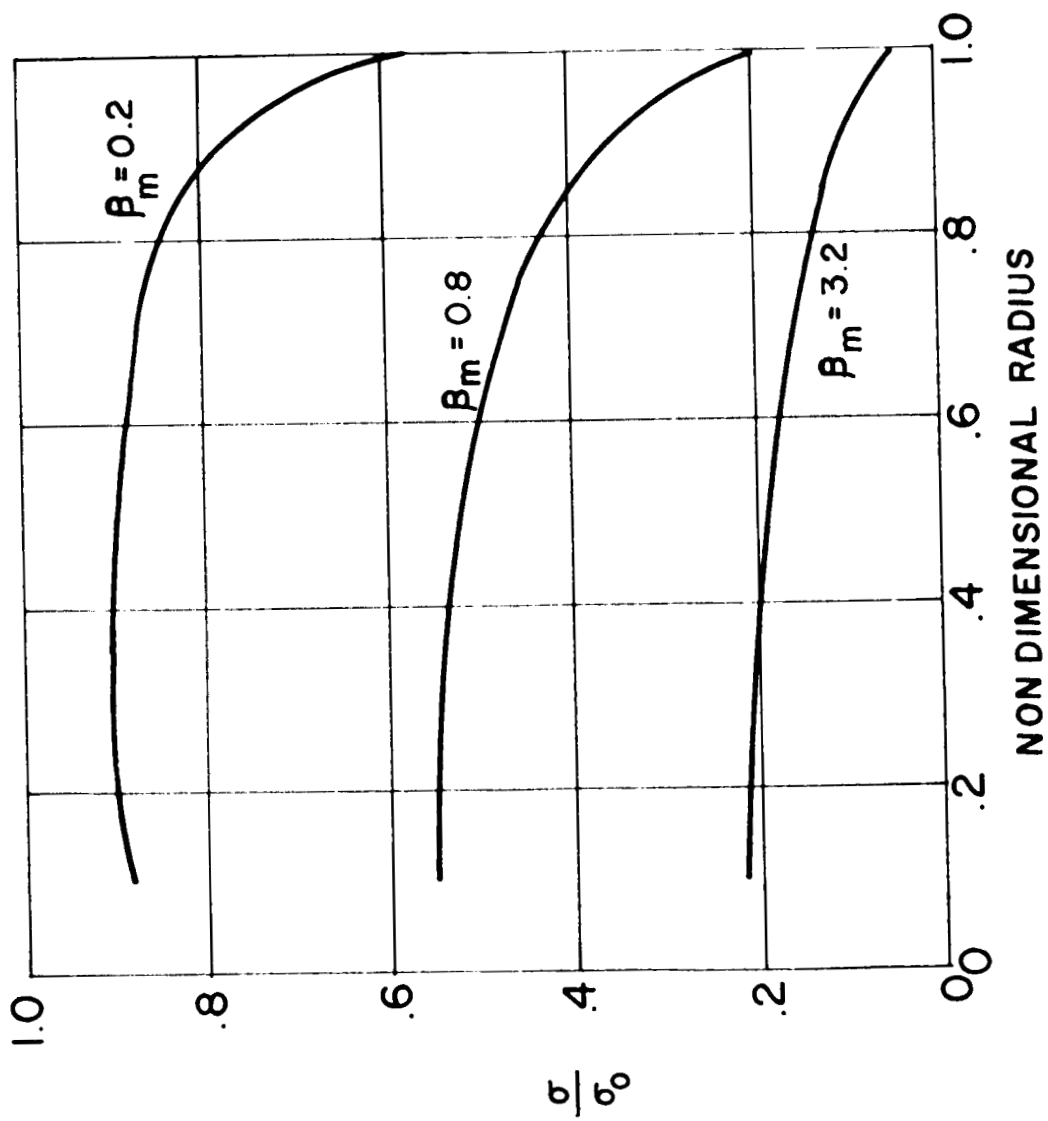


Figure 7:

Vibration of Coning Angle
With Mean Coning Angle, β_m



$$\frac{b}{R} = .1 \quad \ell_m / R = .05$$

$$\gamma_{0t} = 70^\circ \quad \ell_a / \ell_m = 1.0$$

Figure 8: Variation of Fiber Stress with β_m

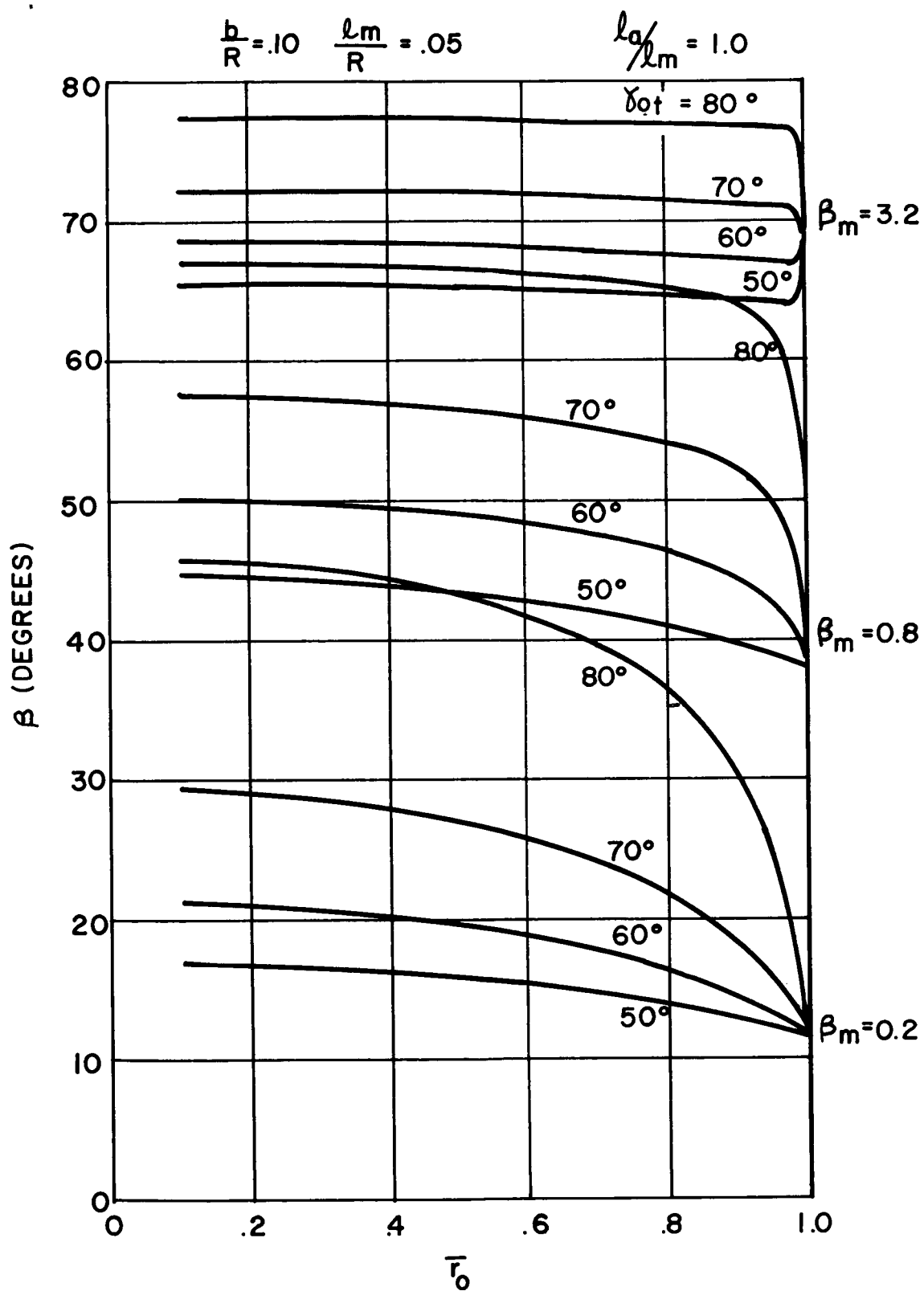


Figure 9: Effect of γ_{0t} on Local Coning Angle

$$\frac{b}{R} = .1 \quad \frac{l_m}{R} = .05 \quad \frac{l_a}{l_m} = 1.0$$

$$\beta_m = .2$$

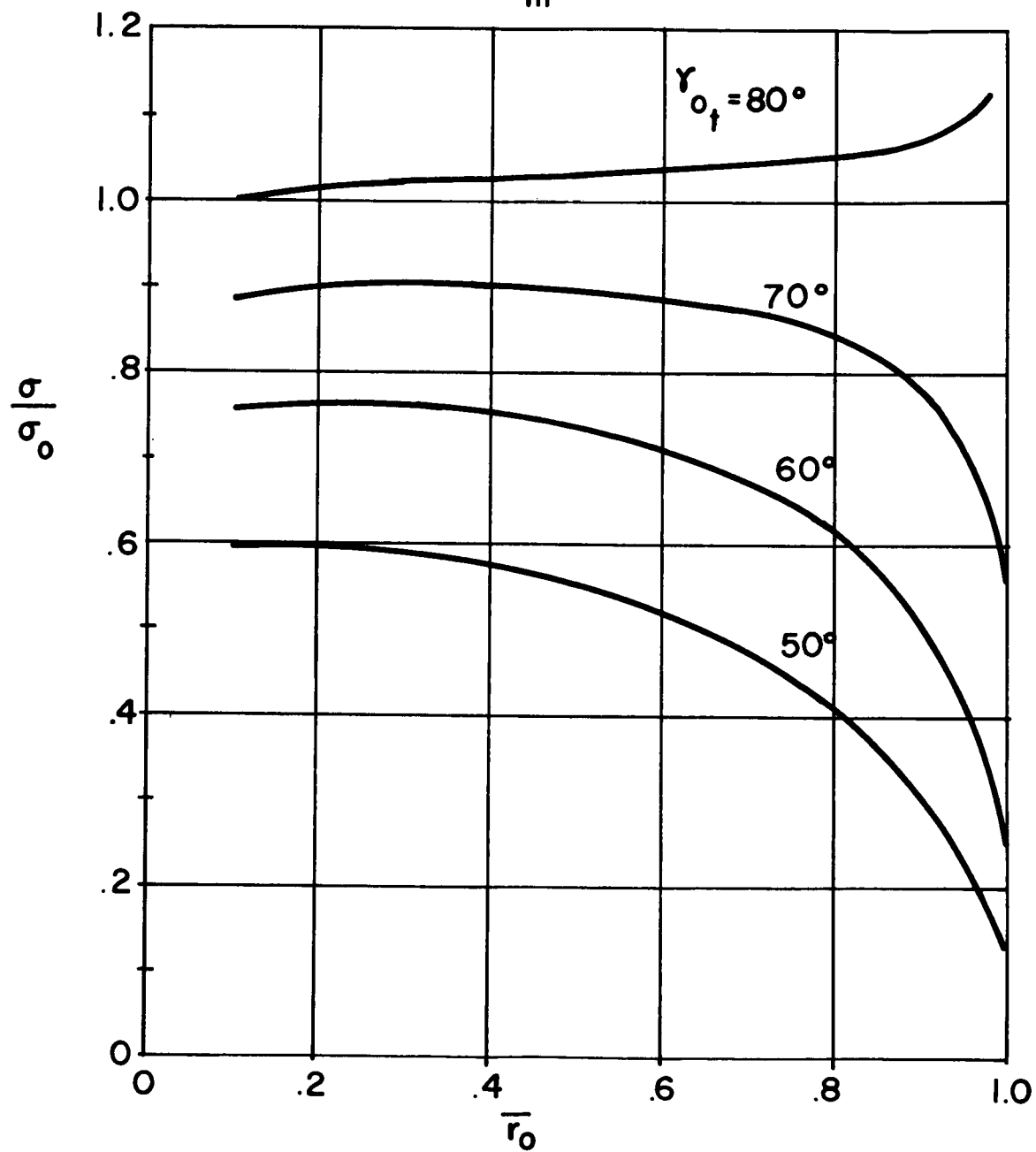
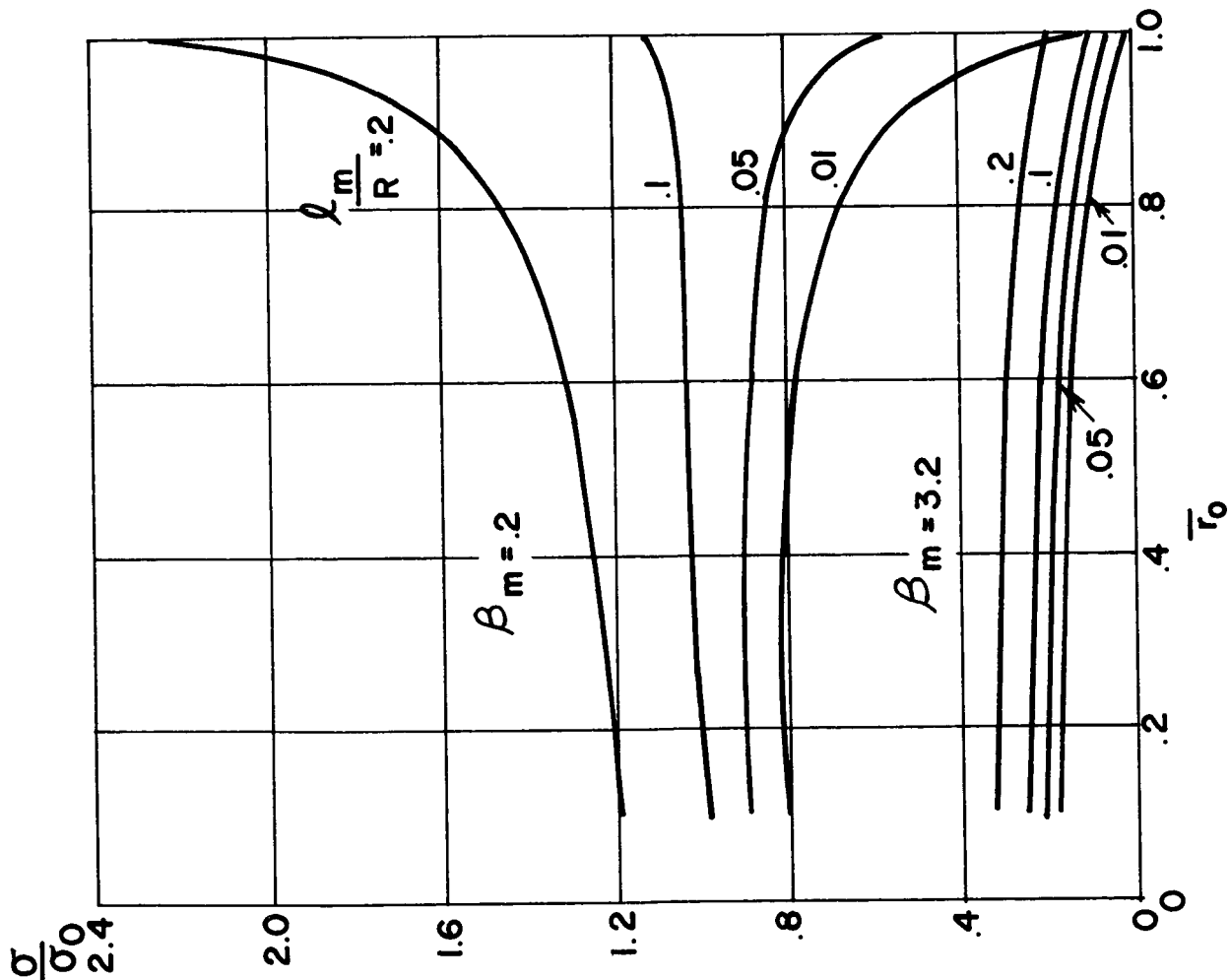


Figure 10: Effect of γ_{ot} on Fiber Stress



$$\sigma_{01} = 70^\circ \quad \frac{b}{R} = .10$$

$$\frac{l_a}{l_m} = 1.0$$

Figure 11: Effect of $\frac{l_m}{R}$ on
Fiber Stress

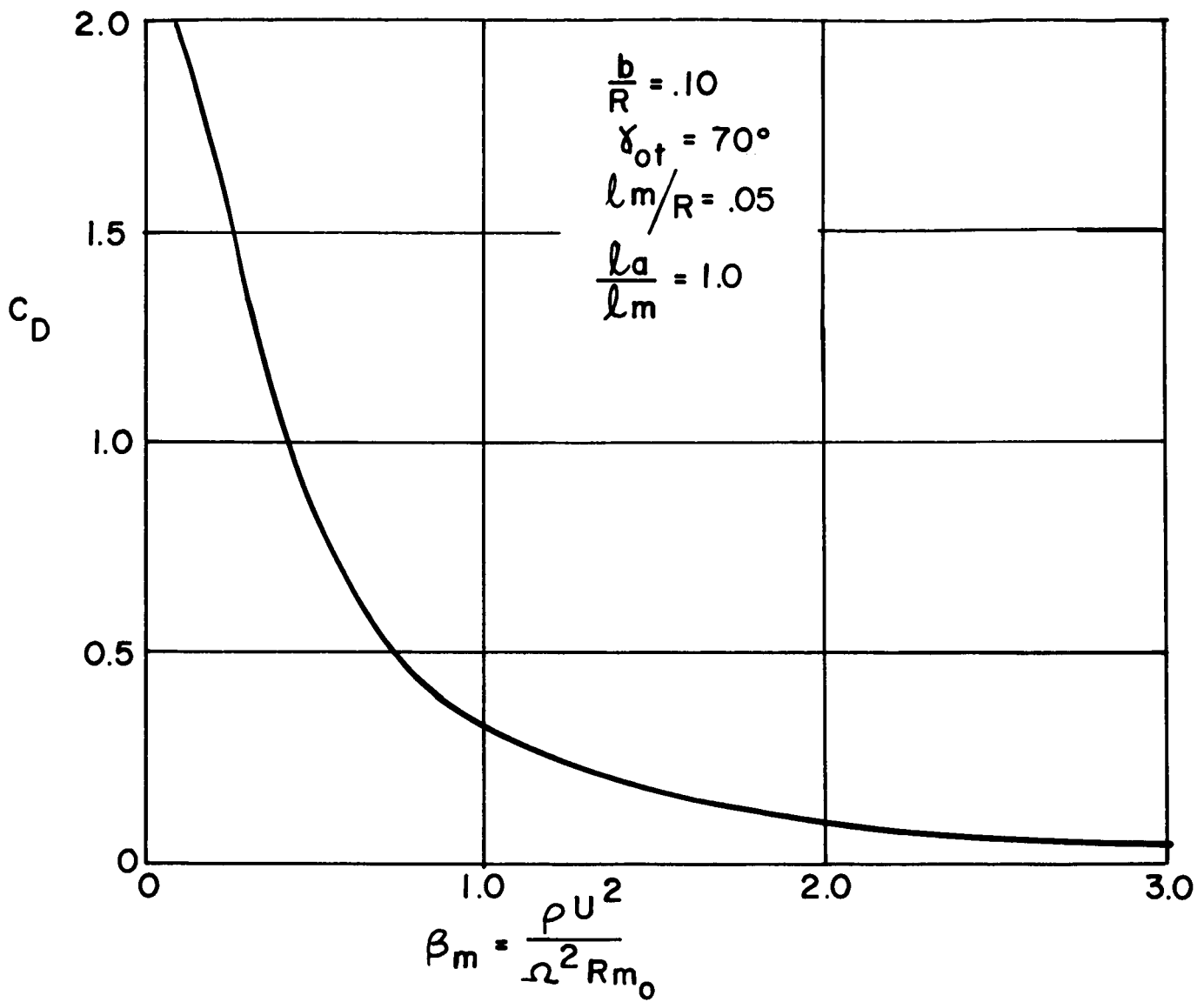


Figure 12: Variation of Drag Coefficient, C_D , With Mean Coning Angle, β_m

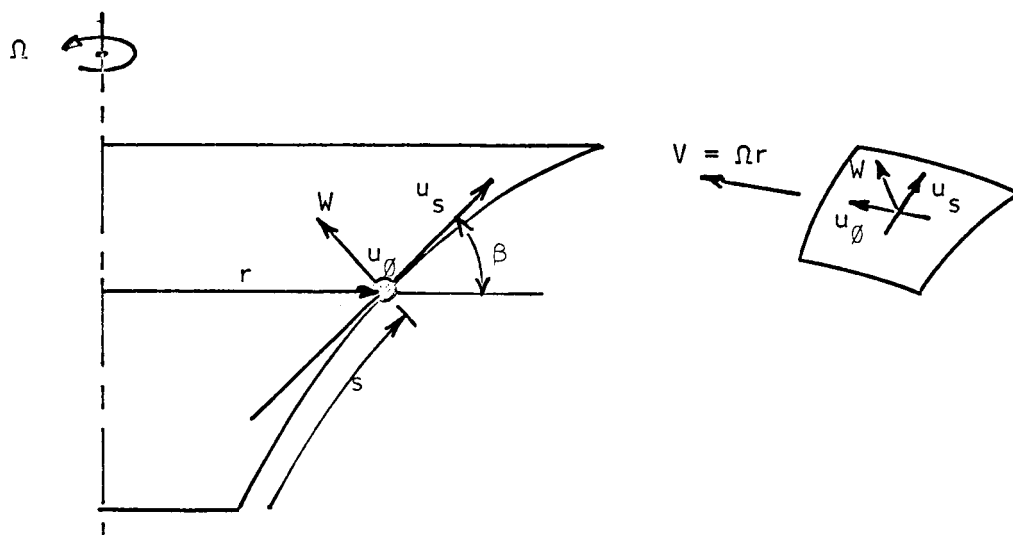


FIG. 13. Displacement Components for Small Motions of an Axisymmetric Net

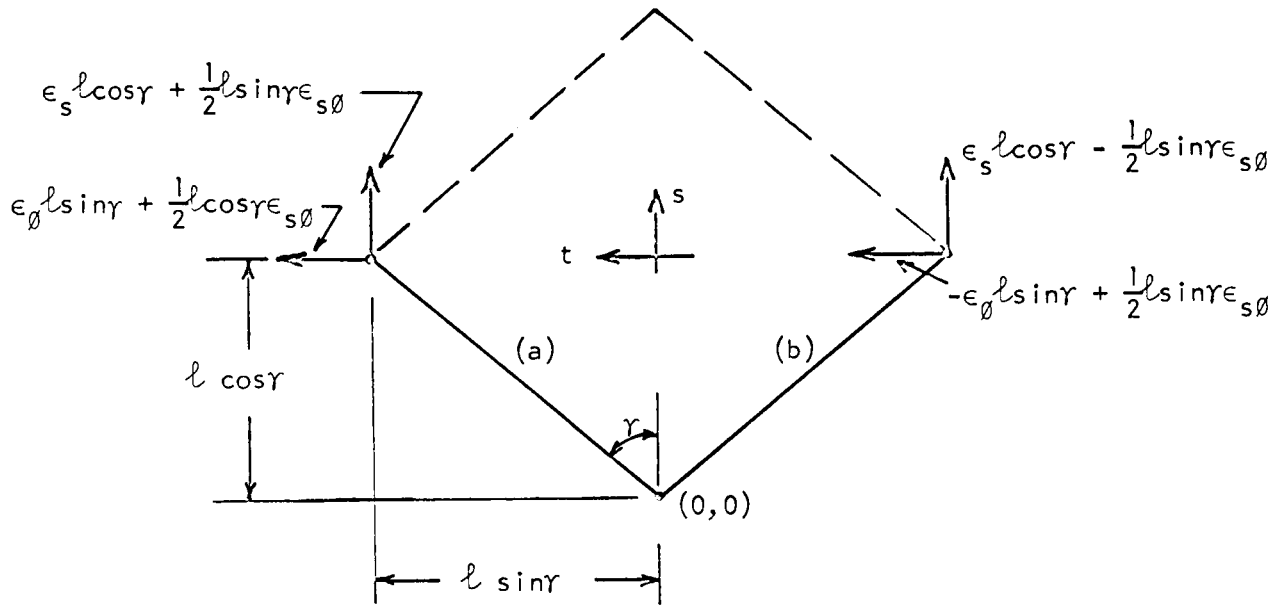


FIG. 14. Elastic Distortion Without Rotation of a Fiber Diamond

$$\left\{ \frac{\partial u_s}{\partial t} = \frac{\partial u_\theta}{\partial s} = \frac{1}{2} \epsilon_{s\theta} \right\}$$

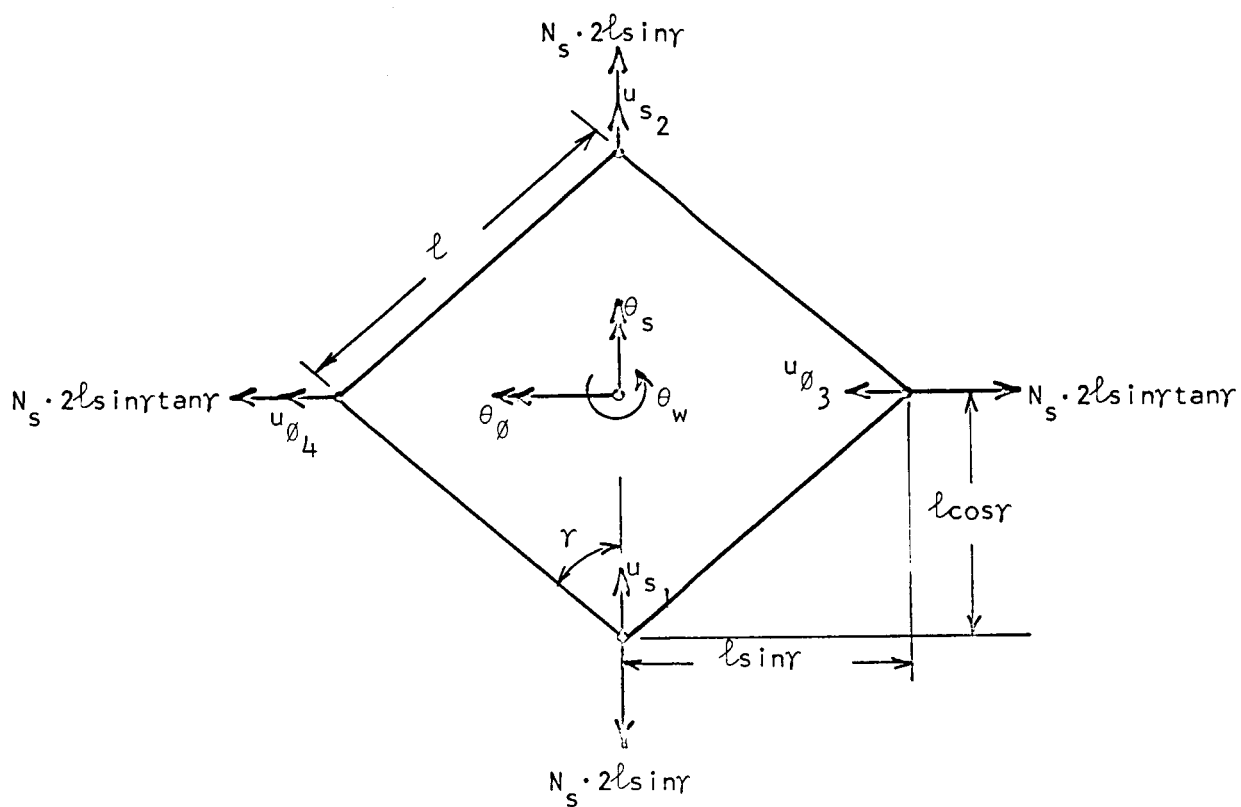


FIG. 15. Static Forces Acting on an Elemental Diamond

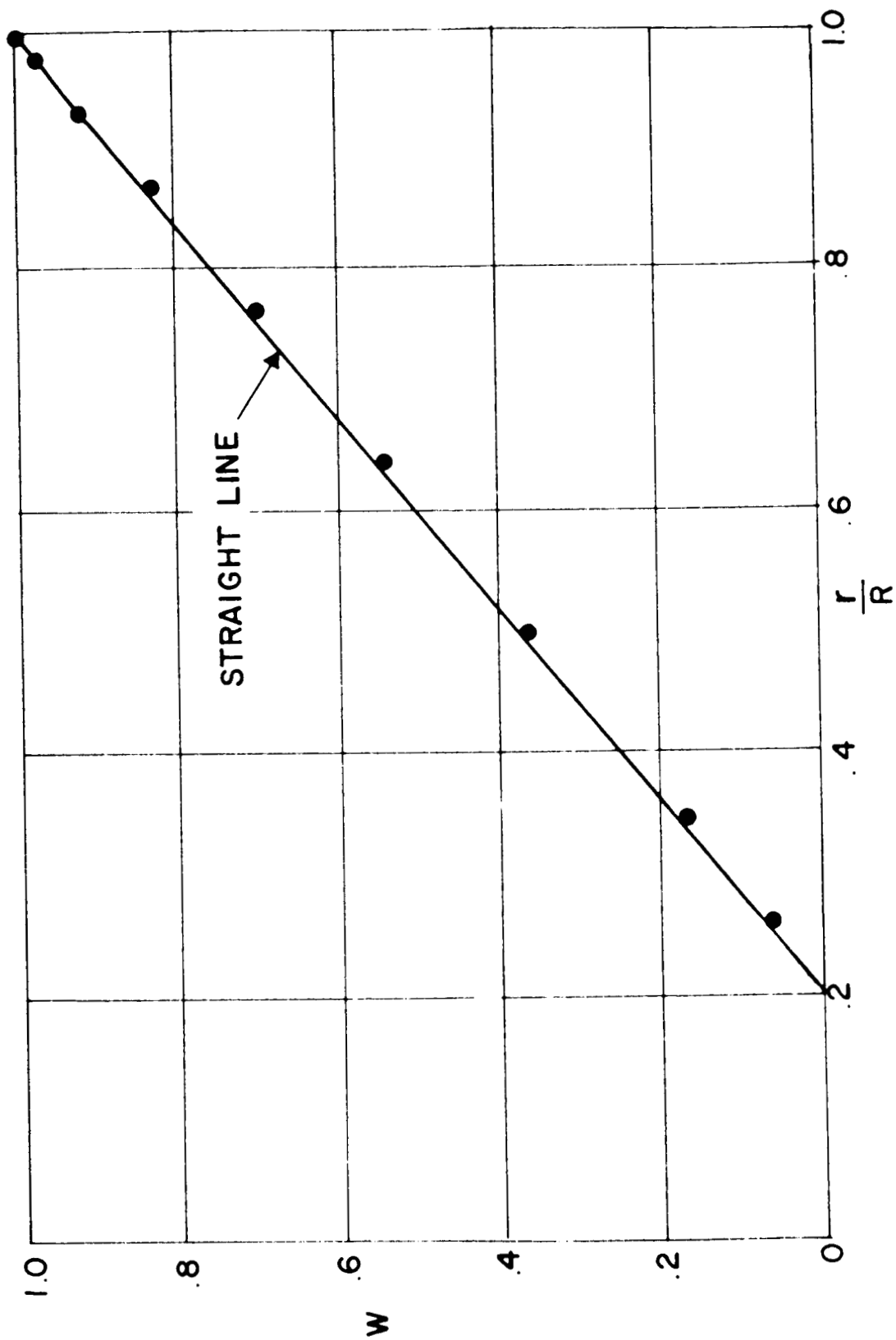


Figure 16: Out-of-plane Vibration of a Flat Isotensoid Net Mode Shape
for $n = 1$, $m = 1$ mode with $b/R = .2$ $\bar{\omega} = 1.076$

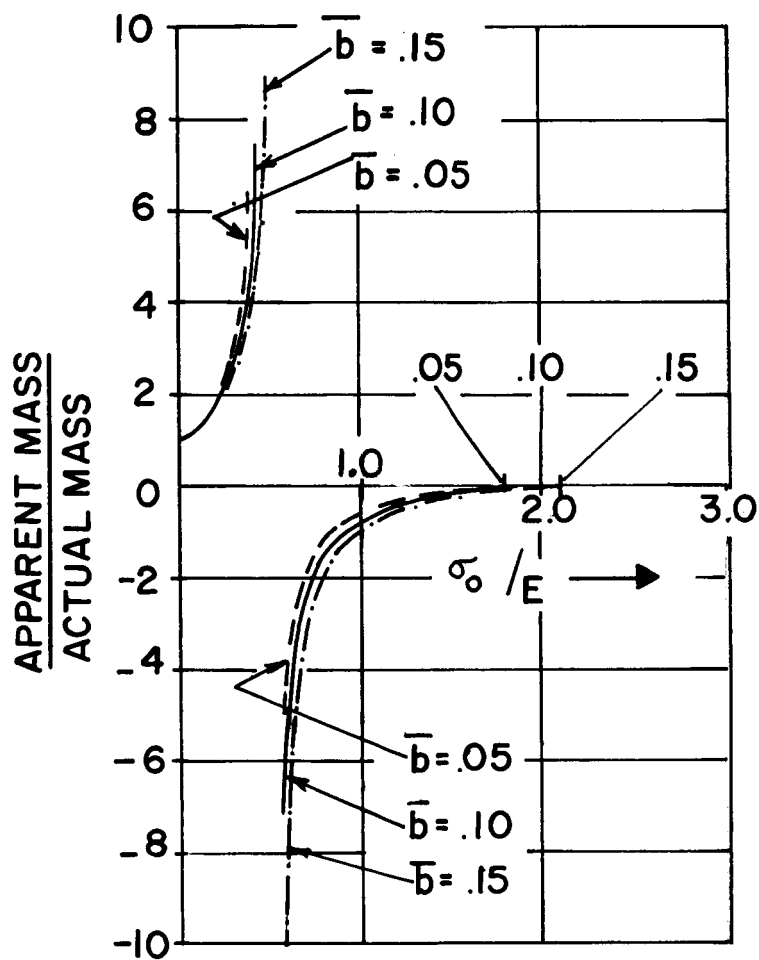


Figure 17: Apparent In-plane Mass of a Rotor Net

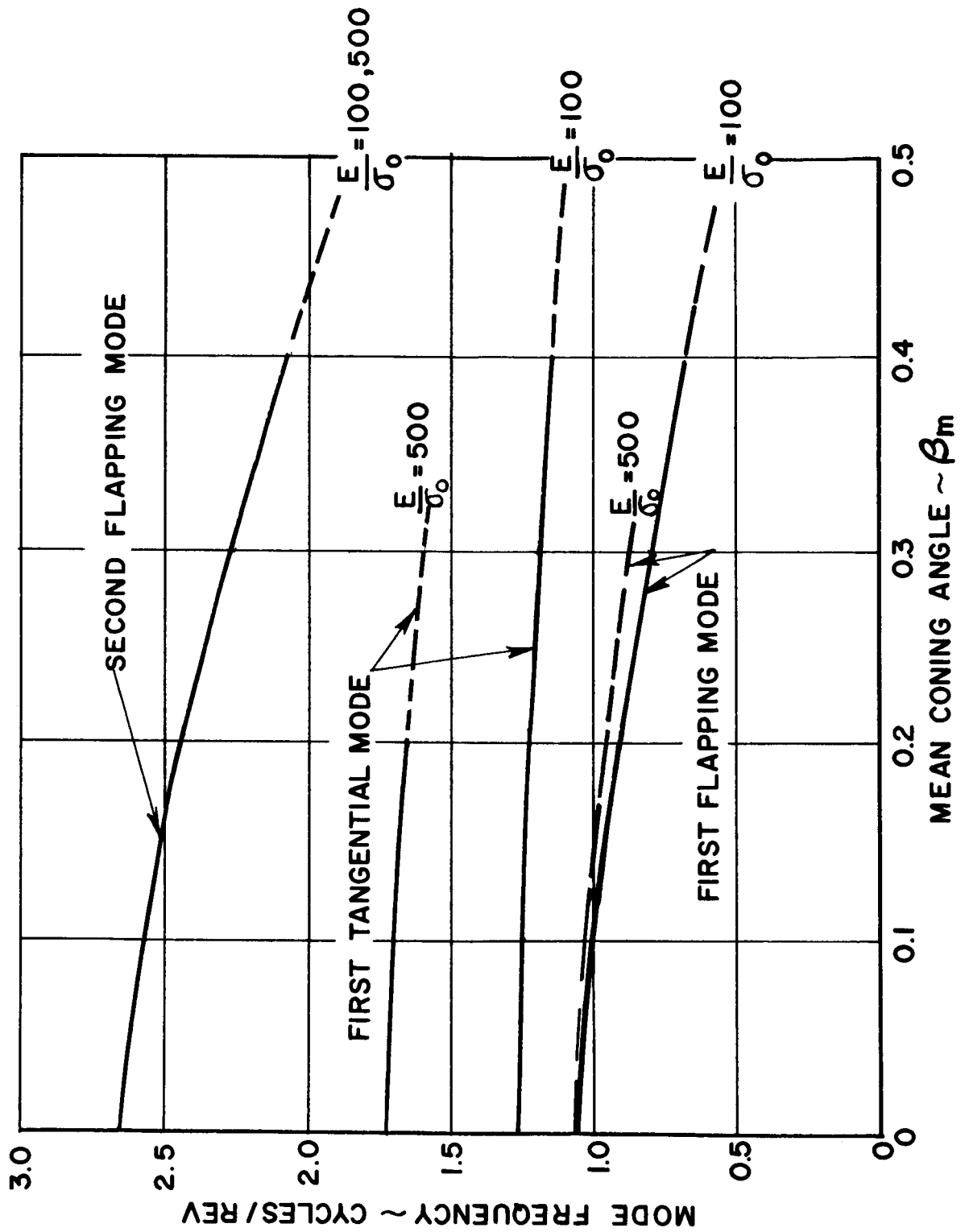


Figure 18: Coned Net Vibration Frequency Summary
 $b/r = 0.1$, $\gamma_{ot} = 70^\circ$, $\frac{l_m}{R} = 0.05$

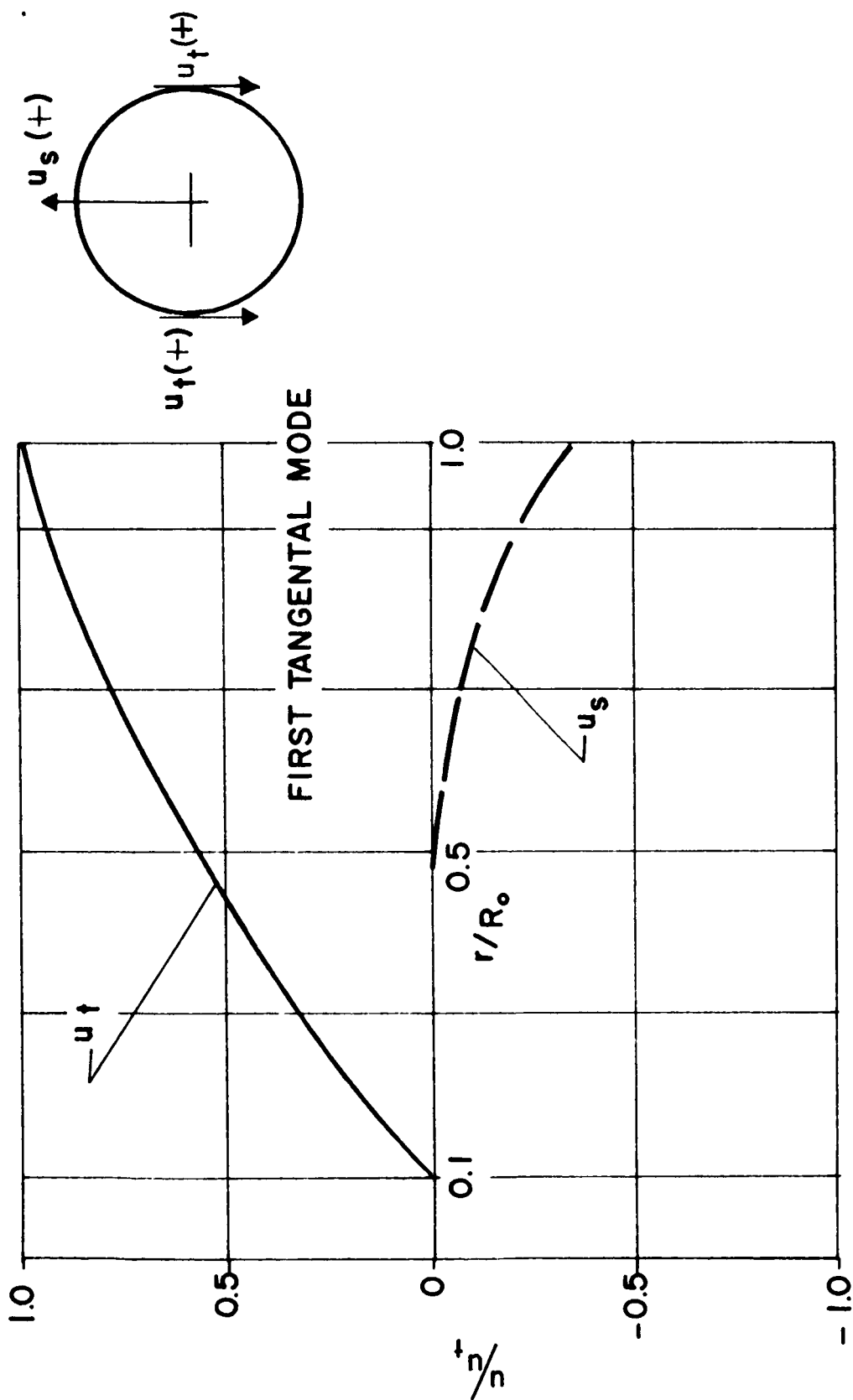


Figure 19: Tangential Mode for Flat Net, $\bar{\omega} = 1.26$
 $\beta_m = 0, E/\sigma_0 = 100$

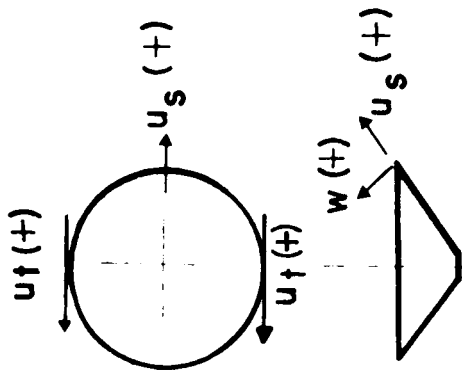
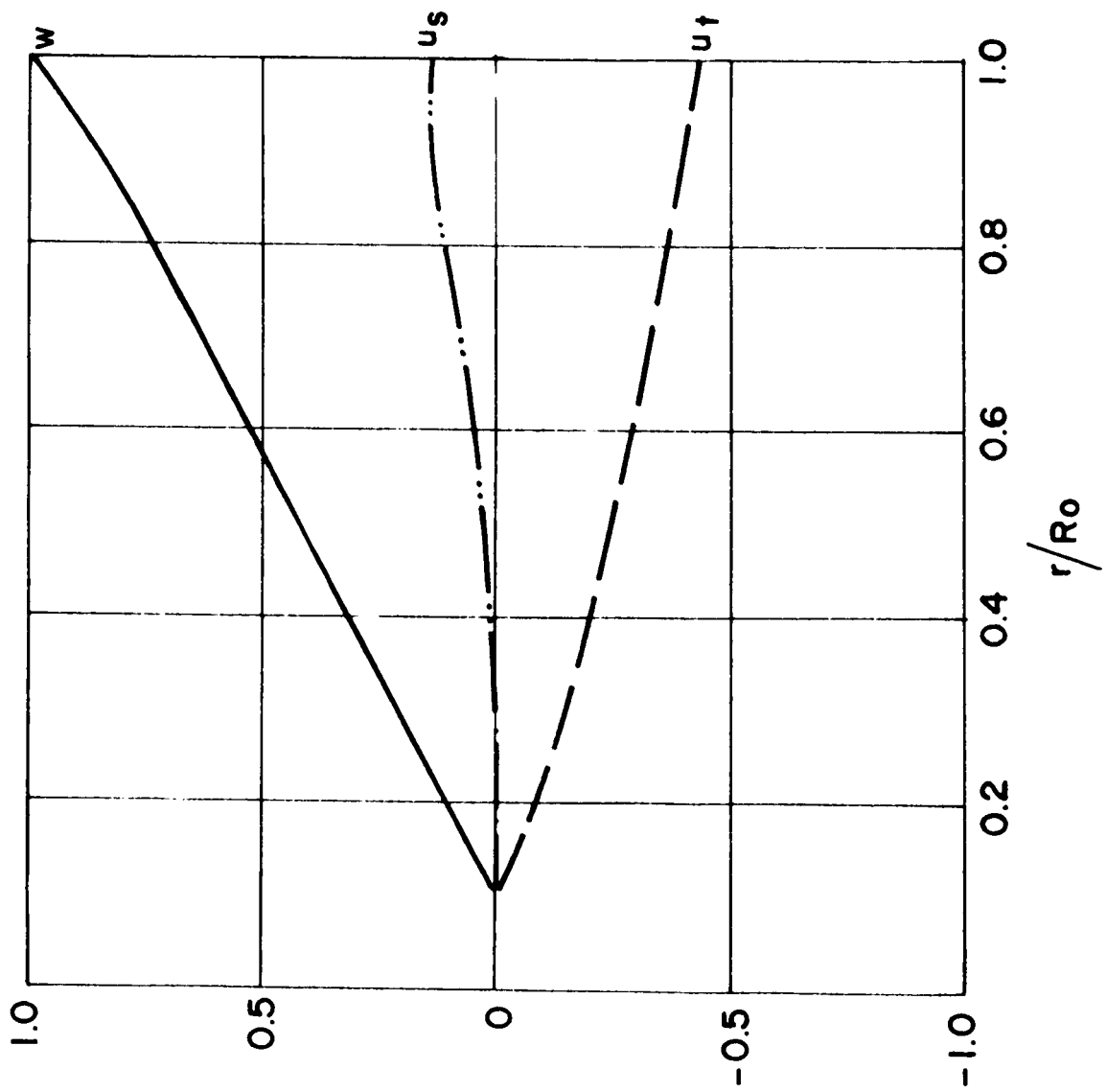


Figure 20: First Flapping Mode $\bar{\omega} = 0.92$
 $\beta_m = 0.2, \frac{E}{\sigma} = 100$

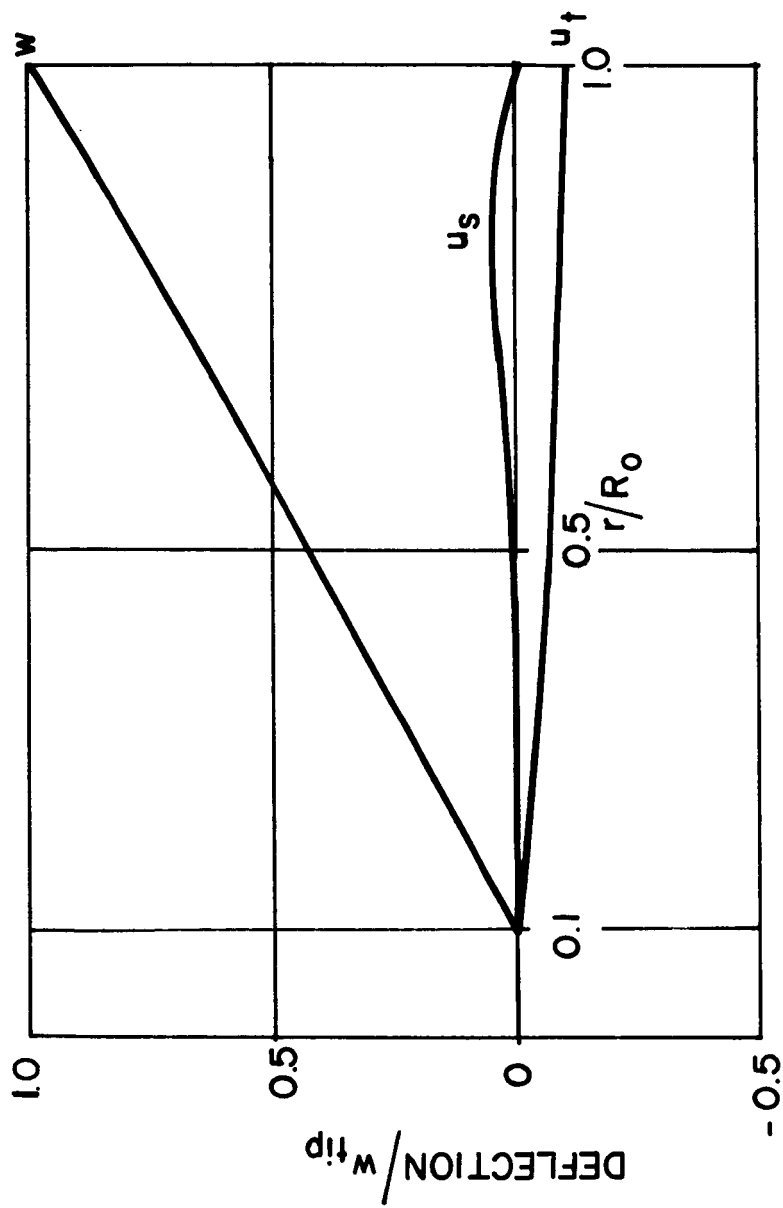


Figure 21: First Flapping Mode $\bar{\omega} = 0.96$
 $\beta_m = 0.2, E/\sigma = 500$

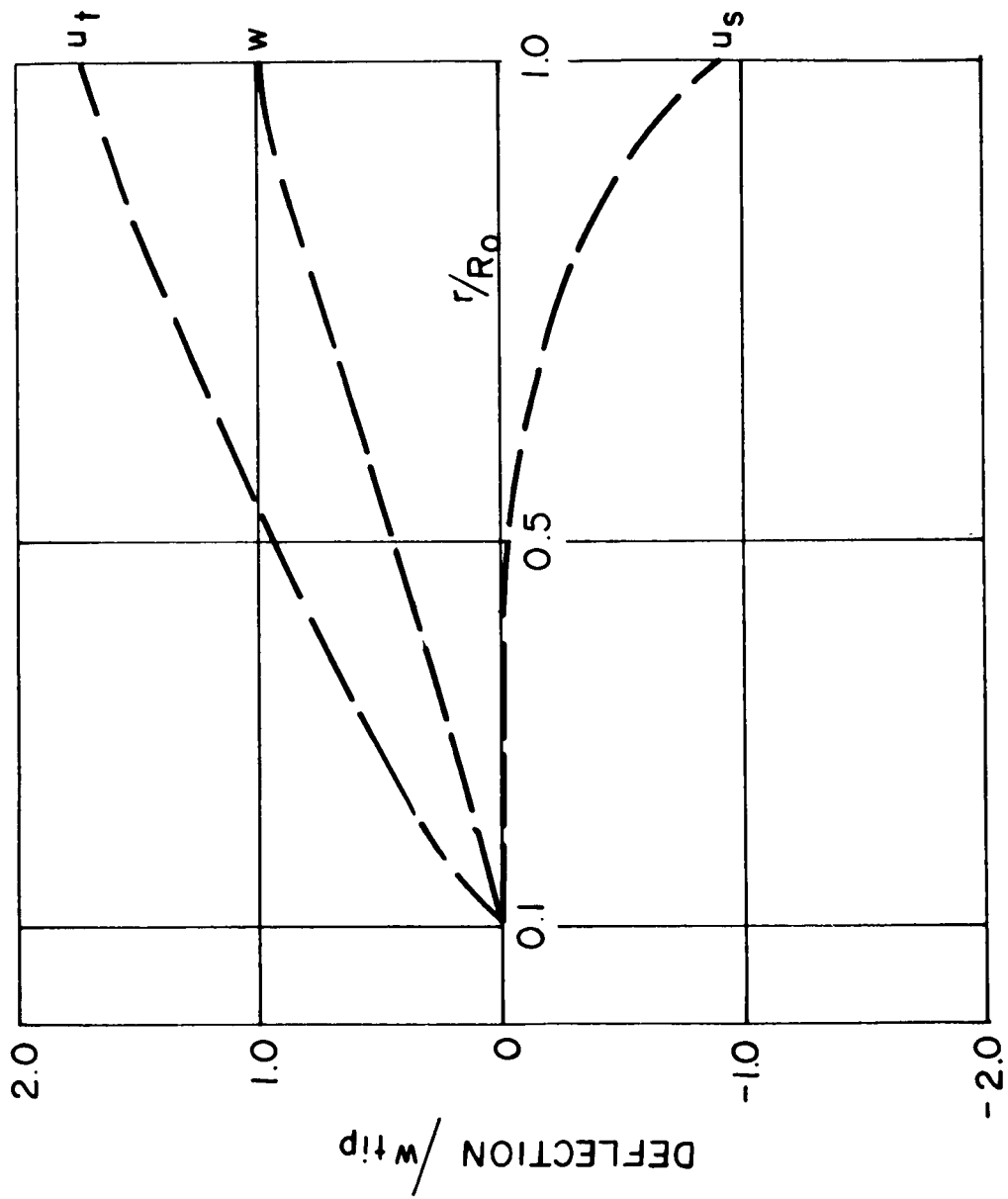


Figure 22: First Tangential Mode $\bar{\omega} = 1.22, \beta_m = 0.2, \frac{E}{\sigma} = 100$

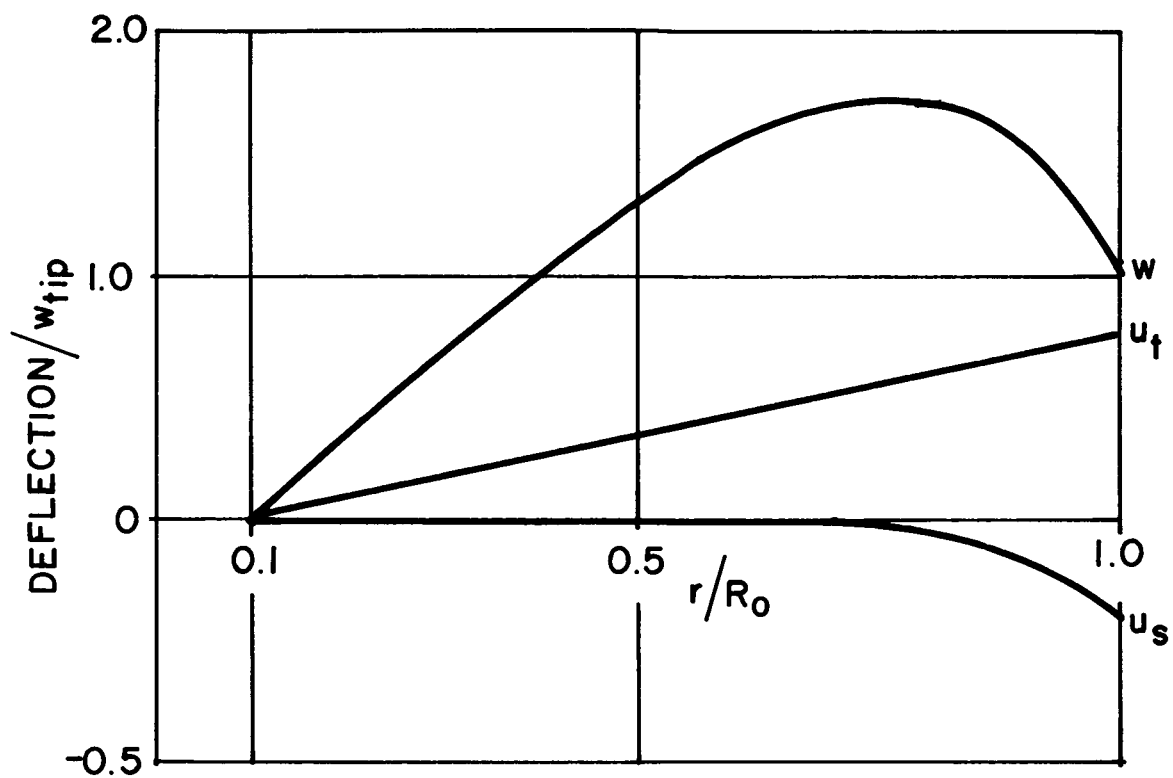


Figure 23: First Tangential Mode $\bar{\omega} = 1.65$
 $\beta_m = 0.2, \frac{E}{\rho} = 500$

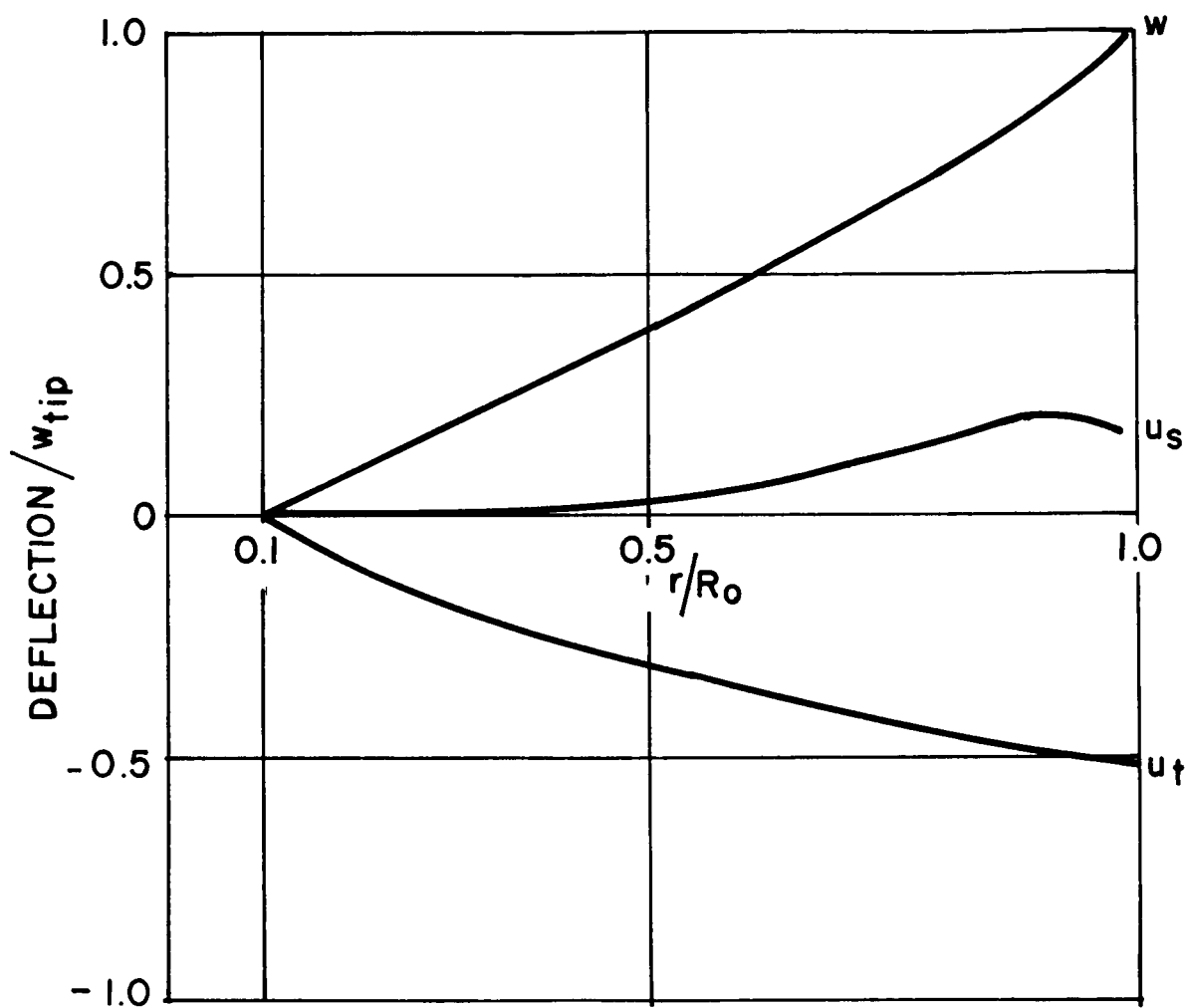


Figure 24: First Flapping Mode $\bar{\omega} = 0.67$
 $\beta_m = 0.4, \frac{E}{\sigma} = 100$

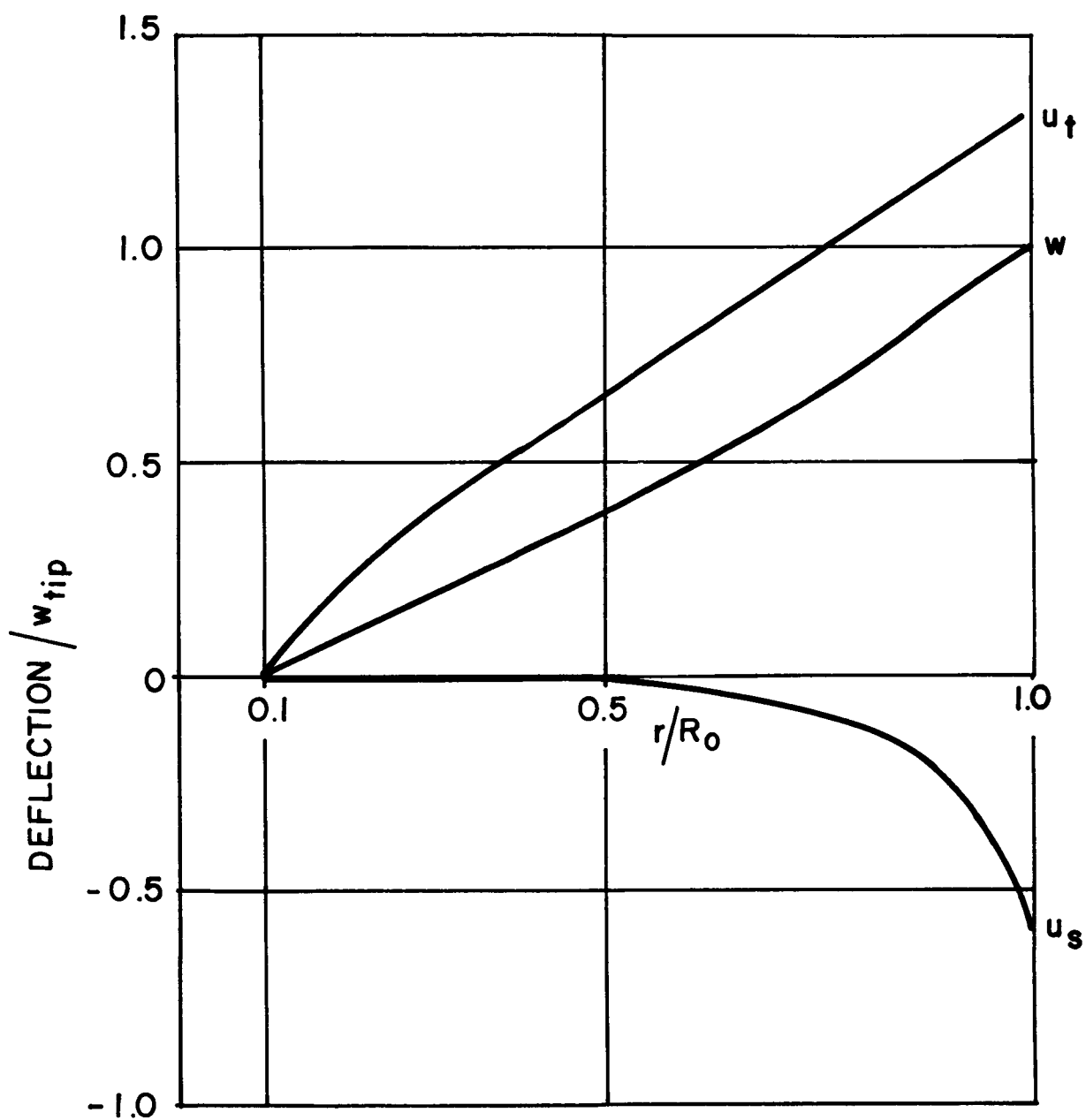


Figure 25: First Tangential Mode $\bar{\omega} = 1.15$
 $\beta_m = 0.4$, $\frac{E}{\sigma} = 100$

A P P E N D I X A

METHOD FOR OBTAINING NUMERICAL SOLUTIONS TO VIBRATION PROBLEMS

In the main text the formulation of vibration problems is carried to the point where integral expressions are written for the kinetic and potential energies. The general procedure that has been used for obtaining solutions is as follows:

1. Approximate the integrals by summations of terms that are functions of displacements at discrete points.
2. Draw a picture of a lumped parameter physical system (in the present case, an electrical network) for which the energy is identical to the expressions obtained in step one and that properly satisfies all boundary conditions.
3. Solve the equations of the lumped parameter physical system on a digital computer.

Electrical networks have been chosen as physical models primarily because of the availability of a digital computer program (SADSAM II) that can solve the equations of any passive electrical network and that accepts input data in a form that is particularly simple to prepare, i.e., a wiring table for the network and a list of element values.

The general procedure will be explained with reference to the problem formulated in section 6. Expressions for elastic energy, the work done against static preload, and kinetic energy are given by Eqns. (6-18),

(6-19) and (6-20). It will be noted that these expressions involve the sums of terms that are proportional to the squares of displacement quantities.

The stored energy of an electrical capacitor is

$$V_C = \frac{1}{2} C e^2 \quad (A-1)$$

where e is the voltage and C is the capacity. Also, for sinusoidally varying voltage, the peak stored energy of an inductor is

$$V_L = \frac{1}{2} \cdot \frac{1}{\omega^2 L} \cdot e^2 \quad (A-2)$$

where e is now the peak voltage, ω is the frequency in radians per second and L is the inductance. Comparing these expressions with Eqns. (6-18), (6-19) and (6-20) it may be seen that V_L may be identified with \bar{V}_e and that V_C may be identified with $\bar{T} - \bar{V}_s$ such that

$$\sum_i V_{L_i} = \bar{V}_e \quad (A-3)$$

and

$$\sum_i V_{C_i} = \bar{T} - \bar{V}_s \quad (A-4)$$

where i and j are summed over all the inductors and capacitors of the equivalent network. Furthermore it is evident by comparing Eqns. (6-18) and (A-2) that the frequency, ω , in the electrical network is analogous to $\sqrt{\frac{\sigma_0}{E}}$. Thus the lowest resonant frequency of the electrical network

- corresponds to the critical value of σ_0/E .

The integral of Eqn. (6-18) shall be replaced by a sum of terms each of which approximates the energy over a short segment, Δr . Consider one such term:

$$\begin{aligned} \Delta \bar{V}_e = \frac{E}{\sigma_0} \Delta r \cos \gamma_t \cos \gamma \cdot \frac{r^2}{2} & \left[\left\{ \frac{\Delta_r \bar{u}_s}{\Delta r} \operatorname{ctn} \gamma + (\bar{u}_s + \bar{u}_\emptyset) \frac{\tan \gamma}{r} \right\}^2 \right. \\ & \left. + \left\{ \frac{\bar{u}_s + \bar{u}_\emptyset}{r} - \frac{\Delta_r \bar{u}_\emptyset}{\Delta r} \right\}^2 \right] \quad (A-5) \end{aligned}$$

where the finite difference operator $\Delta_r/\Delta r$ replaces $\partial/\partial r$. Comparing the result with Eqn. (A-2) it is seen that $\Delta \bar{V}_e$ may be represented by the energy of two inductors. For the first inductor

$$\frac{1}{L_1} = \Delta r \cdot \cos \gamma_t \cos \gamma \cdot r^2 \quad (A-6)$$

$$e_1 = \frac{\Delta_r \bar{u}_s}{\Delta r} \operatorname{ctn} \gamma + (\bar{u}_s + \bar{u}_\emptyset) \frac{\tan \gamma}{r} \quad (A-7)$$

and similarly for the second inductor.

In the network \bar{u}_s and \bar{u}_\emptyset are represented by voltages with respect to ground at a number of points along the radial coordinate as shown in Fig. A-1. The voltage e_1 in Eqn. (A-7) is obtained by adding such voltages together in proper proportions. Ideal transformers are used for the purpose as shown in Fig. A-1.

Following the above procedure for all of the other energy terms a complete electrical network representation of the problem is obtained. A typical cell of the final network is shown in Fig. A-2.

The properties of the network can be investigated with a passive analog computer, see reference 3, or with a digital computer as in the present instance.

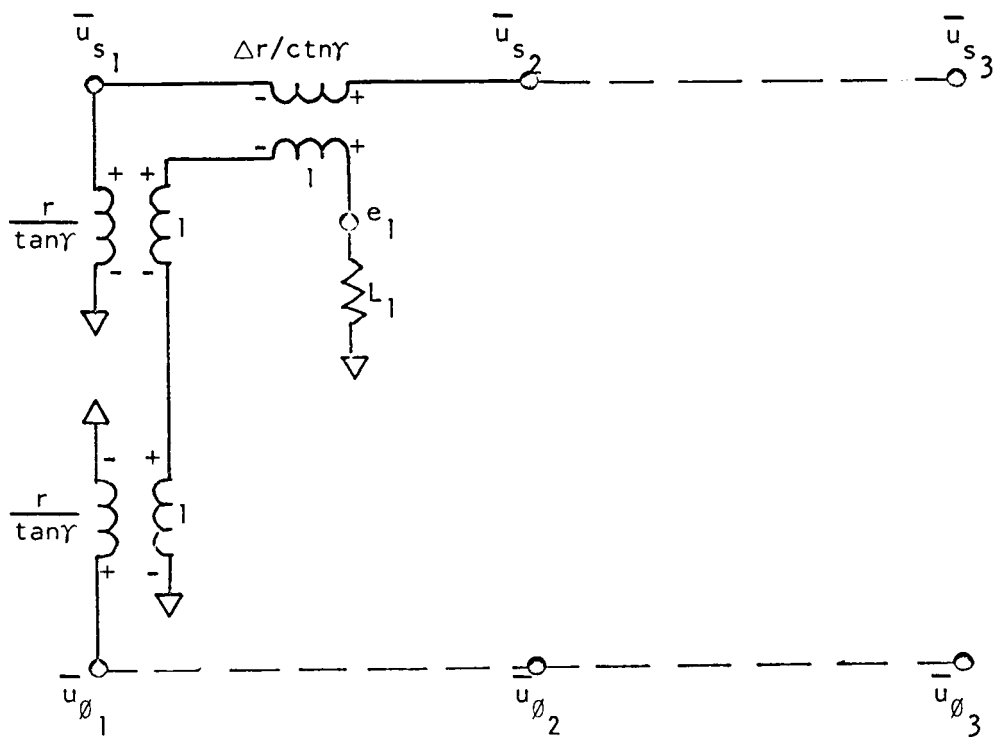
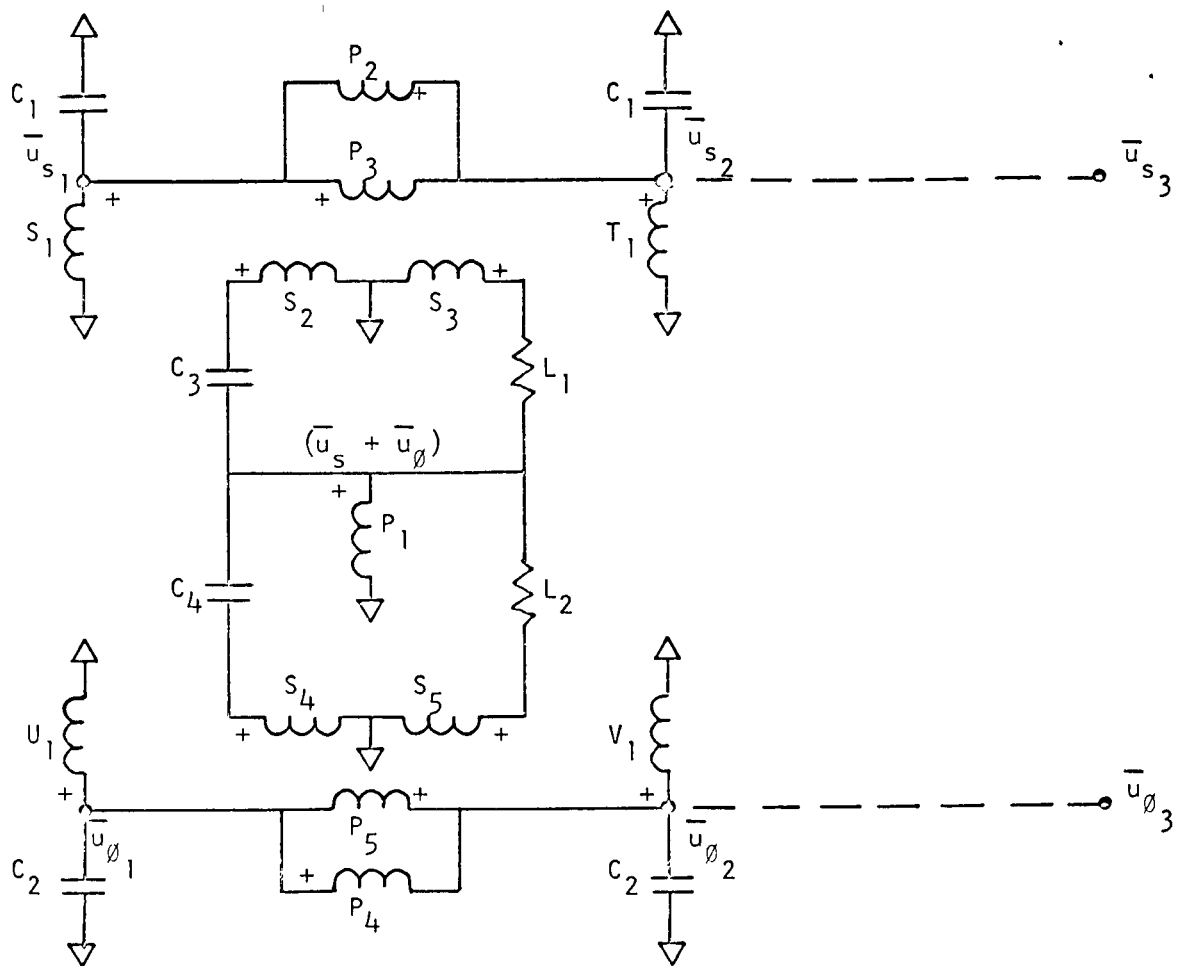


FIG. A-1. Circuit for Simulating the First Term of $\Delta \bar{V}_e$, Eqn. (A-5)



$$C_1 = C_2 = 2 \cos \gamma_t \Delta r / \cos \gamma$$

$$C_3 = -a^2 \cos \gamma_t \tan^2 \gamma \Delta r / r^2 \cos \gamma$$

$$C_4 = -a^2 \cos \gamma_t \Delta r / r^2 \cos \gamma$$

$$\frac{1}{L_1} = \cos \gamma_t \cos \gamma \tan^2 \gamma \Delta r$$

$$\frac{1}{L_2} = \cos \gamma_t \cos \gamma \Delta r$$

T_1 is a multi-core transformer

$$\frac{P_1}{S_1} = \frac{P_1}{T_1} = \frac{P_1}{U_1} = \frac{P_1}{V_1} = \frac{1}{2}$$

$$\frac{P_2}{S_2} = \frac{\Delta r}{r} \tan^2 \gamma$$

$$\frac{P_3}{S_3} = \frac{\Delta r}{r} \tan^2 \gamma$$

$$\frac{P_4}{S_4} = \frac{\Delta r}{r}$$

$$\frac{P_5}{S_5} = \frac{\Delta r}{r}$$

FIG. A-2. Typical Cell of Complete Circuit for In-Plane Vibration Problem